ESTIMATION AND ADAPTIVE EQUALIZATION OF COMMUNICATIONS CHANNELS

BY KARTHIK SRIDHAR DHARMARAJAN

A thesis submitted to the

Graduate School—New Brunswick

Rutgers, The State University of New Jersey

in partial fulfillment of the requirements

for the degree of

Master of Science

Graduate Program in Electrical and Computer Engineering

Written under the direction of

Professor David G. Daut

and approved by

_____

_____

_____

_____

New Brunswick, New Jersey

January, 2015

ABSTRACT OF THE THESIS

Estimation and Adaptive Equalization of Communications Channels

by Karthik Sridhar Dharmarajan

Thesis Director: Professor David G. Daut

The focus of this research is to determine the channel impulse response of a communications link and then equalize the channel to mitigate the effects of fading on the received signal. Traditionally, channel identification is achieved using a deconvolution process implemented in the time-domain. An alternative method is to perform deconvolution, for the purpose of estimating communications channel structures, in the wavelet transform domain. This approach is attractive for use in agile transceivers that utilize the wavelet domain for functions such as automatic modulation recognition. An equivalent method for deconvolving discrete time-domain signals within the Discrete Wavelet Transform (DWT) framework is explained. This method of deconvolution can be applied at any level of DWT resolution from which the complete channel impulse response can be estimated. Computer simulations have been conducted to characterize the performance of the channel estimation algorithm using the Mean Square Error (MSE) criterion. The simulation experiments are performed for two different channel models characterized by a Power Delay Profile (PDP), i.e., the Gaussian PDP and the Exponential PDP. Channel conditions of slow and fast fading are considered. In addition, the faded channel output signals are corrupted by AWGN having ratios of

bit energy-to-noise spectral density, E_b/N_0, in the range from 0 to 30 dB. It has been found that, for both channel models, the best channel impulse response estimate is obtained from the DWT detail coefficients at the first level of resolution resulting in computational efficiency.

A novel method, based on the classic LMS algorithm, has been developed for adaptive equalization of channels in the wavelet domain. Computer simulation experiments for channel equalization show that the DWT-LMS algorithm, using a Haar wavelet, performs better than the LMS algorithm for the Gaussian PDP channel in terms of the achievable bit error probabilities.

Acknowledgements

I would like to thank my advisor Professor David G. Daut, ECE Department, Rutgers University for providing me with his valuable guidance and help throughout the course of this research. This project could not have been accomplished without his assistance. I would like to thank my fellow graduate students, Mr. Yao Ge and Ms. Tejashri Kuber for helping me in difficult situations. I am grateful to Professor Sophocles Orfanidis and Professor Zoran Gajic for serving on my Masters Thesis Committee and for their evaluation of my thesis research work. I greatly appreciate their valuable contribution! Lastly, I thank my family and friends for believing in me throughout the course of my graduate studies. Your relentless support has been very important for me.

Table of Contents

Abstract ii

Acknowledgements iv

List of Figures vii

1. Introduction 1

1.1. Motivation 1

1.2. Objectives 3

1.3. Thesis Organization 4

2. Theoretical background 6

2.1. Multipath channels 6

2.1.1. Characteristics of fading multipath channels 6

2.1.2. Fading effects of multipath channels 7

2.2. Adaptive Equalization 9

2.2.1. Operating modes of an adaptive equalizer 11

2.3. The Least Mean Squares algorithm 11

2.3.1. Method of steepest descent 12

2.3.2. Filter weight derivation for LMS algorithm 15

2.3.3. Properties of LMS algorithm 15

2.3.3.1. Gradient behavior 16

2.3.3.2. Convergence behavior of coefficient vector 16

3. Literature survey 20

3.1. Wavelet analysis 20

3.2. Wavelet background 20

3.2.1. Basics of Wavelets . . . 21
3.2.2. Haar and Daubechies wavelets . . . 22
3.3. Discrete Wavelet Transform . . . 24
3.4. Discrete Wavelet Transform-based Channel Estimation . . . 29
3.5. Discrete Wavelet Transform-based Adaptive Equalization . . . 31

4. Technical preliminaries . . . 33
4.1. Mutiresolution analysis and subband coding . . . 33
4.2. Convolution in discrete wavelet domain . . . 38
4.2.1. Noble identities of Multirate filters . . . 39
4.3. Forward Merge approach . . . 41

5. DWT-based channel estimation . . . 45
5.1. Deconvolution using DWT . . . 45
5.2. Computer simulation experiments . . . 49
5.2.1. Experimental procedure . . . 50
5.3. Results . . . 51
5.3.1. Channel 1: Gaussian power delay profile . . . 51
5.3.2. Channel 2: Exponential power delay profile . . . 54

6. Discrete wavelet transform-based adaptive equalization . . . 57
6.1. Equalization using DWT . . . 57
6.2. Strategy for DWT-based adaptive equalization . . . 57
6.3. Computer simulation experiments . . . 58
6.4. Results . . . 59
6.4.1. Channel 1: Slow fading Gaussian power delay profile . . . 59
6.4.2. Channel 2: Slow fading Exponential power delay profile . . . 63
6.5. Observations . . . 67

7. Conclusions . . . 68
7.1. Summary . . . 68
7.2. Future work . . . 70

List of Figures

1.1. Components of a communication system. 2

2.1. Adaptive Equalization block diagram. 10

3.1. Haar wavelet. 23

3.2. db2 wavelet. 24

3.3. Filter analysis block diagram [1]. 25

4.1. Two-channel subband coding analysis and synthesis [1]. 34

4.2. M channel Filter bank [1]. 39

4.3. Filtering followed by downsampling [1]. 39

4.4. The first identity [1]. 40

4.5. Filtering followed by upsampling [1]. 40

4.6. The second identity [1]. 40

4.7. Basic Convolution. 41

4.8. Level-1 DWT and IDWT of $R(z)$ [1]. 41

4.9. Forward merge approach of DWT convolution [1]. 42

4.10. Original 2-level DWT/IDWT filter bank [1]. 43

4.11. Modified 2-level DWT/IDWT filter bank [1]. 43

4.12. Forward Merge approach at two levels of DWT [1]. 44

5.1. DWT convolution of $X(z)$ and $Y(z)$ [1]. 46

5.2. DWT and IDWT of $R(z)$ [1]. 47

5.3. Gaussian PDP for fast fading. 52

5.4. Gaussian PDP for slow fading. 52

5.5. Channel impulse response estimation errors for the fast fading Gaussian power delay profile case; Haar wavelet. 53

5.6. Channel impulse response estimation errors for the fast fading Gaussian power delay profile case; Db2 wavelet. 53
5.7. Channel impulse response estimation errors for the fast fading Gaussian power delay profile case; Db3 wavelet. 54
5.8. Channel impulse response estimation errors for the fast fading Gaussian power delay profile case; Db4 wavelet. 54
5.9. Exponential channel PDP for slow fading. 55
5.10. Exponential channel PDP for fast fading. 55
5.11. Channel impulse response estimation errors for the fast fading Exponential power delay profile case; Haar wavelet. 56
5.12. Channel impulse response estimation errors for the slow fading Exponential power delay profile case; Haar wavelet. 56
6.1. Strategy for DWT-based adaptive equalization. 58
6.2. Gaussian power delay profile for delay spread of 3 seconds. 60
6.3. Error probability vs SNR for LMS and DWT-LMS equalizers using the Haar wavelet in Gaussian PDP channel. 61
6.4. Error probability vs SNR for LMS and DWT-LMS equalizers using db2 wavelet in Gaussian PDP channel. 61
6.5. Error probability vs SNR for LMS and DWT-LMS equalizers using db3 wavelet in Gaussian PDP channel. 62
6.6. Error probability vs SNR for LMS and DWT-LMS equalizers using db4 wavelet in Gaussian PDP channel. 62
6.7. Exponential PDP for RMS delay spread of 3 seconds. 63
6.8. Error probability vs SNR for the LMS and DWT-LMS equalizers using the Haar wavelet in Exponential PDP channel. 64
6.9. Error probability vs SNR for the LMS and DWT-LMS equalizers using db2 wavelet in Exponential PDP channel. 65
6.10. Error probability vs SNR for the LMS and DWT-LMS equalizers using db3 wavelet in Exponential PDP channel. 66

6.11. Error probability vs SNR for the LMS and DWT-LMS equalizers using db4 wavelet in Exponential PDP channel. 66

Chapter 1

Introduction

Wireless communication has become increasingly important not only for professional applications but also for many activities in our daily routine and in the consumer electronics industry. In recent years, wireless communication technology has been delivering high data speeds, and it provides a relatively low cost, high-quality services. With the development of advanced wireless communication technology, new services have been developing [1] [2].

Various modern communication systems employ time, frequency and spatial multiplexing techniques to achieve the various goals of efficient communication. A new platform shall be developed for the interoperability of all current and emerging standards. One of such platform is that of reconfigurable, or agile radios where signals can be transmitted using different modulation schemes on different carrier frequencies and then be identified and demodulated using advanced Automatic Modulation Recognition(AMR) schemes at the receiver. Recently, automatic modulation recognition schemes have been developed using Wavelet transforms. However, two vital elements for the functioning of an agile transceiver system are Channel Estimation and Channel Equalization. Hence, this thesis research is dedicated towards developing new channel estimation and equalization techniques within a wavelet platform which later can be combined with Wavelet-based Automatic Modulation Recognition methods [3].

1.1 Motivation

The major components of a communication receiver are shown in Figure 1.1:

an RF front-end;

a Mixed signal stage; and finally a data demodulator

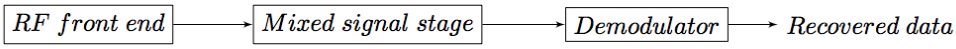

Figure 1.1 Components of a communication system.

The receiver RF-front end consists of antenna up to, and including the first digital baseband system. It consists of a bandpass filter (BPF) to eliminate out of band signals and an RF amplifier to amplify the signal strength. It also consists of a local oscillator or mixer which is used to convert a signal of interest to an intermediate frequency. This process of frequency conversion is called heterodyning which produces sum and different frequencies resulting from the frequency of the local oscillator and the frequency of the input signal of interest. The Mixed signal stage downconverts the signal processed by the front-end for use in baseband digital receivers. Finally, the demodulator is used for extracting the original information from the received waveform [2].

The Fourier transform is used to represent the frequency content of a signal, i.e., how much of each of the frequencies exist in the signal. Also it is a reversible transform, it can switch back and forth between time-domain and frequency-domain signal representations. But the disadvantage of this transform is that a finite duration signal cannot be represented in both time and frequency domains accurately at once. It does not give information about the time-varying behavior of the frequency content. In most practical applications almost all signals are non-stationary. Hence, the Fourier transform cannot accurately be applied on real-time signals that are observed for short durations [4].

As an alternative, the Short Time Fourier Transform (STFT) can be employed to divide the non-stationary signal into chunks of small time duration stationary signals using finite width window signals. Finally, a Fourier transformation can be applied on these chunks of relatively stationary signals. But for good stationarity the window size should be small resulting in diminished frequency resolution. Hence, a signal analysis approach

which has a variable window size is desired [5] [6].

Wavelets can be both temporally translated and dilated in time. This specific feature allows for variation in the window width so as to give the desired frequency resolution besides making the windowed signal chunk stationary. Hence, in this thesis research the wavelet transform will be used to process digitally modulated signals that are input to an agile receiver. In particular, Channel Estimation and Equalization techniques will be investigated in terms of their implementation and performance when a wavelet domain signal processing approach is employed.

1.2 Objectives

The following are the major objectives of this research study:

1. To determine the time domain impulse response of a communications channel using wavelet transforms and to implement algorithms for wavelet-based channel estimation.

2. To equalize the fading effects of a communications channel on the signal using the wavelet transform and implement a novel algorithm for wavelet-based channel equalization. A Discrete Wavelet Transform (DWT) approach will be used in adaptive equalization.

Channel Estimation

In channel estimation, the channel impulse response coefficients are estimated using pilot signals and then the actual signals are transmitted. A pilot signal is transmitted and a copy of the same signal is available at the receiver. Using these two signals, one corrupted and the other uncorrupted, the communications channel impulse responses can be estimated. Here, the concept of deconvolution can be applied where the received distorted signal is deconvolved with the already existing copy at the receiver. In this work, deconvolution is applied employing wavelets and the performance is compared with time-domain channel estimates.

An analytical formulation of DWT-based deconvolution is to be developed, and it is to be validated using computer simulations. The simulations are performed using a Monte-Carlo method. The simulation experiments are performed for two channel models and two fading cases for each channel. The Haar, db2, db3, and db4 wavelets are used for channel estimation and their relative performance is compared.

Channel Equalization

Linear equalization is one of the equalization procedures which minimizes the fading effects of a communications channel, but this does not adapt to the changes in the channel. Adaptive equalization is primary method used in real world scenarios. Here, the concept is to minimize the error between the input and the output data symbols. This implies that the output shall be made as close as to the input. Here the main aim is to minimize the error function to be as close to zero as possible.

The Lease Mean Squares (LMS) algorithm is one of the classic adaptive algorithms for the equalization of channels. In this research study, a DWT-based LMS algorithm is developed for adaptive equalization of channels in the Wavelet domain. The simulation experiments are performed for two channel PDP models and use four different wavelet families per channel. Monte Carlo simulations are performed to assess the algorithm performance. Comparison is made between the traditional LMS algorithm results and the newly developed DWT-based LMS algorithm results.

1.3 Thesis Organization

The research study first focuses on Wavelet transform domain convolution which is basis for the development of the two main objectives namely - wavelet-based channel estimation and equalization. Hence, the major topics of the research study are as follows:

1. Convolution in the Discrete Wavelet Transform (DWT) domain

2. DWT-based channel estimation

3. DWT-based channel equalization

Following the Introduction, the theoretical concepts of various prerequisite communication concepts are explained in Chapter 2. It includes the concepts of multipath channels and their fading effects. The theory behind the adaptive equalization algorithm, i.e., the Least Mean Squares algorithm, is explained in Chapter 2.

A comprehensive survey of the technical literature relevant to the research topics is presented in Chapter 3. These concepts include wavelet transforms, multiresolution analysis and the prior work done in the area of channel estimation and equalization involving wavelets.

The method of convolution in the discrete wavelet domain is emphasized in Chapter 4. Specifically, an equivalent convolution method is analytically derived using the identities and explained with the aid of illustrations. The equivalent is method named the Forward Merge approach. It is used as a basis for the developments in the subsequent chapters.

DWT-based channel estimation is developed and results are discussed in Chapter 5. Two different channel models are explored. Also in Chapter 5, the criteria for the experiments such as channel models, test signal generation and the procedure of experiments are explained. Similarly, DWT-based channel equalization is focused on in Chapter 6. The well known LMS adaptive equalization algorithm is implemented in the wavelet domain and performance results are presented.

The thesis is concluded in Chapter 7 with a summary of the research results. The recommended future research topics are included which can be an extension to the work performed in this study.

Chapter 2

Theoretical background

The formal definitions of channels used in this thesis and in the general context of communications, is included in this chapter. Characterization of multipath channels including the various aspects of fading is described in Section 2.1. Various available equalization procedures used to combat the ill effects of ISI are explained in Section 2.2.

2.1 Multipath channels

Signals that propagate through wireless media are subject to many effects like distortion, dispersion and reflection from the objects in its path. Hence, the signal received at the receiver is said to be a faded signal if the received signal power is attenuated over any, or all, of the channel bandwidth. Channels that cause this fading effect are called fading channels. Often, there are multiple copies of the transmitted signal at the receiver. These fading channels are termed as multipath channels [1].

2.1.1 Characteristics of fading multipath channels

Let a sinusoid be transmitted through a multipath channel. The received signal is

$$r_l(t) = \sum_n \alpha_n(t) e^{-j2\pi f_c \tau_n(t)} \tag{2.1}$$

$$r_l(t) = \sum_n \alpha_n(t) e^{-j\theta_n(t)} \tag{2.2}$$

where $\theta_n(t) = 2\pi f_c \tau_n(t)$. Here, $\alpha_n(t)$ is the attenuation factor for the n^{th} path and $\tau_n(t)$ is the propagation delay for the same path.

It can be seen from (2.1) that when $\tau_n(t)$ changes by a factor of $1/f_c$ the phase of the n^{th} received sinusoid changes by a factor of 2π. Hence, small changes in the channel can cause significant changes to the phase of the signal transmitted.

For the received signal $r_l(t)$ to be modeled as a random process, the assumption made is that $\tau_n(t)$'s of various paths are independent and change randomly. This implies that the impulse response of the channel can be modeled as a complex Gaussian process [1] [3].

Rayleigh fading channel

A channel is said to be a Rayleigh fading channel if the channel does not possess a Line of Sight path. In this case the channel impulse response can be characterized as a zero-mean Gaussian random process. The complex envelope of the channel will have a Rayleigh distribution [1].

Rician fading channel

When a Line of Sight component does exist in the medium, then the received signal is composed of a dominant signal component as well as scatterers. In this case, the complex envelope is Rice distributed [1].

2.1.2 Fading effects of multipath channels

The following assumptions are made to explore the fading effects of multipath channels. The first assumption is that the impulse response of channel is Wide Sense Stationary (WSS) [1] [4].

1. Mean is constant, i.e.,

$$E\{x(t)\} = E\{x(t+\tau)\} \quad \forall \ t \in \mathbb{R} \tag{2.3}$$

2. The autocorrelation function, $R_x(t_1, t_2)$ depends only on difference between time instants t_1 and t_2

$$R_x(t_1, t_2) = R_x(t_1 + \tau, t_2 + \tau) = R_x(t_1 - t_2, 0) \ \ \forall \ \ t \in \mathbb{R} \tag{2.4}$$

In keeping with the assumption of WSS for channels considered in this study, the autocorrelation function is defined as [1] [3]

$$\phi_c(\tau_1, \tau_2; \Delta t) = \frac{1}{2} E\left\{c^*(\tau_1; t) c(\tau_2; t + \Delta t)\right\} \tag{2.5}$$

The second assumption is that the attenuation and phase in any two different paths are uncorrelated. This type of multipath propagation is called **Uncorrelated scattering** [1]. If the autocorrelation function is evaluated for $\Delta t = 0$ it is simply $\phi_c(\tau)$ which is average power output of channel when excited by an impulse and is called the **Power Delay Profile** (PDP) of the channel [1] [4]. The autocorrelation of the transfer function of the channel can be expressed as

$$\phi_c(f_1, f_2; \Delta t) = \frac{1}{2} E\left\{C^*(f_1; t) C(f_2; t + \Delta t)\right\}. \tag{2.6}$$

Invoking the definitions of $G(f)$ in the Fourier domain gives

$$\phi_c(f_1, f_2; \Delta t) = \frac{1}{2} \int_{-\infty}^{\infty} \int_{-\infty}^{\infty} E\left\{c^*(\tau, t) c(\tau_2; t + \Delta t)\right\} e^{j2\pi(f_1\tau_1 - f_2\tau_2)} d\tau_1 d\tau_2 \tag{2.7}$$

$$\phi_c(f_1, f_2; \Delta t) = \int_{-\infty}^{\infty} \phi_c(\tau_1; \Delta t) e^{j2\pi\Delta f \tau_1} d\tau_1 = \phi_c(\Delta f; \Delta t) \tag{2.8}$$

Here, Δf is called the **Coherence bandwidth** of the channel. If the bandwidth of the transmitted signal is less than this coherence bandwidth then the channel is said to be **Flat Fading** channel. On the other hand if the signal bandwidth is greater than this coherence bandwidth then it is said to be a **Frequency selective channel** [1].

The parameter T_m, called the coherence time of the channel denotes the range of time delay over which the PDP of the channel is non-zero.

$$(\Delta f) = \frac{1}{T_m} \tag{2.9}$$

The duration of time between observations of channel impulse response to be non-varying is called the channel coherence time denoted by $(\Delta t)_c$. If the channel coherence time is shorter than the symbol period of the transmitted signal, i.e., $(\Delta t)_c < T_s$, **fast-fading** occurs. On the other hand **Slow fading** occurs [1] [3] [7].

2.2 Adaptive Equalization

The channel distortion results in ISI causing high error rates. The solution to overcome the problem of ISI in the received signal is to build better receiver structures. This can be done by including a compensator called an equalizer in the receiver structure which compensates for the imperfect channel response $G(f)$ resulting in ISI in the received signal.

There are two types of equalizers - a fixed Linear equalizer and a non-fixed or Adaptive equalizer. Linear equalizer makes use of linear filters to compensate the effects of channel distortion and to estimate the transmitted information sequence. The Zero-Forcing equalizer is one of the linear equalization algorithms that uses a peak distortion criterion. It applies the inverse of the channel frequency response to the received signal in order to restore the original transmitted signal. The disadvantage of this method is that, in the case where the received signal is weak, as a result of which the magnitude of the Zero-Forcing filter gain grows very large. This can result in the amplification of any noise present in the signal. Ideally the Zero Forcing equalizer eliminates all the ISI in noise free channels. Unfortunately in practice, there is no completely noise free channel.

In the previous paragraph we have discussed the concept of a Zero Forcing equalizer. The model assumes that the input to the channel results in an output $y(t)$ that is sampled at nT to produce discrete-time sequences $y_n = y(nT)$. The output is now fed into the equalizer with weights w_n to make the resultant look like a unit impulse response or

Kronecker delta function i.e., $y(n) * w(n) = \delta(n)$. Unfortunately, this requires keeping track of channel impulse responses to know if it changes significantly [8].

Adaptive equalization can be a solution for those situations wherein the channel characteristics are time-varying. Adaptive equalizers compensate for signal distortion attributed to intersymbol interference (ISI), which is caused by multipath within time-dispersive channels. Typically, the equalizers are employed in high-speed communication systems, which do not use differential modulation schemes or frequency division multiplexing. The basic idea behind an adaptive equalizer filter is to approach the optimum filter weights by updating the filter weights in a manner so as to converge to the optimum filter weight. The algorithm starts by assuming small weights (zero in most cases), and at each step, by finding the gradient of the mean-squared error, the weights are updated. That is, if the MSE-gradient is positive, it implies, the error would keep increasing positively, if the same weight is used for further iterations, which means we need to reduce the weights. In the same way, if the gradient is negative, we need to increase the weights. This closeness is specified by the well-known error function, the mean-squared error i.e., $e_n^2 = (y_n - x_n)^2$, where $y(n)$ is the equalized output at each iteration and $x(n)$ in the transmitted signal sequence. The aim of an Adaptive Equalization process is to make the error function as close to zero as possible for all n [8] [9].

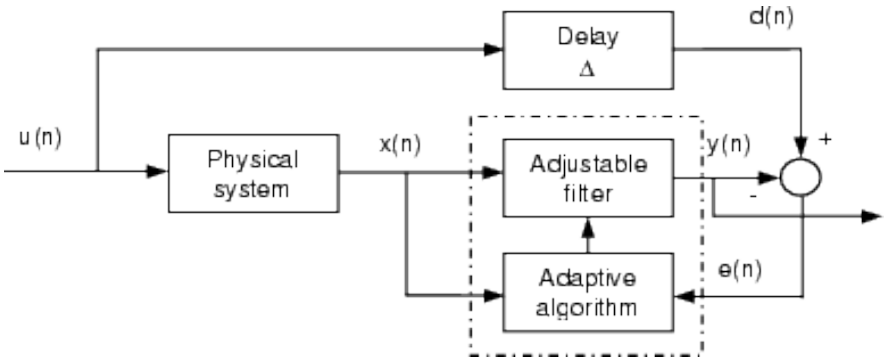

Figure 2.1 Adaptive Equalization block diagram.

Figure 2.1 shows the basic block diagram of an adaptive equalizer. Here, the adaptive filter reaches the optimal weights by minimizing the error between the transmitted

input signal sequence and the equalized output signal at each iteration.

2.2.1 Operating modes of an adaptive equalizer

The two modes are namely the *training mode* and *tracking mode*. In the training mode, a known sequence is input to the equalizer so that the receiver's equalizer may adapt to proper setting. The training sequence is a psuedo-random sequence or a fixed, prescribed bit pattern [8] [9]. The training sequence is designed to permit an equalizer at the receiver to acquire the proper filter coefficients in the worst possible channel conditions. Therefore, when the training sequence is finished, the filter coefficients are near their optimal values for reception of user data. An adaptive equalizer at the receiver uses a recursive algorithm to evaluate the channel and estimate filter coefficients to compensate for the channel. In the tracking mode, the equalizer algorithm after receiving the channel output signal continuously keeps a track of the changing channel, so as to modify the adaptive filter weights and satisfy the minimum error criterion. As a result, the equalizer constantly changes the filter coefficients over time [8] [9].

2.3 The Least Mean Squares algorithm

The least mean squares algorithm is employed by adaptive equalizers in order to find the best filter coefficients that produces smallest error signal in the mean square sense. It is a stochastic gradient descent method which means the filter is adapted only based on the error at the current time. Hence, as the channel changes, the error changes and thereby the algorithm keeps updating the filter coefficients [8].

The basic idea of the LMS algorithm is to approach the optimal filter design by a step-step update of filter weights that converges to their optimum values. The algorithm starts of by choosing small values for the filter weights, and at each step the weights get updated by finding the gradient of the mean square error and updating them. The basic weight adaption equation is

$$W_{n+1} = W_n - \mu\Delta\epsilon[n] \tag{2.10}$$

where, ϵ is the mean square error and μ is the constant step size for controlling the accuracy and speed of weight adaptation. The negative sign indicates that we need to change the weights in the direction opposite to that of the gradient slope. The mean-squared error, as a function of filter weights is a quadratic function which means it has only one extrema, that minimizes the mean-square error, which corresponds to the optimal filter weights. The LMS algorithm thus, approaches the optimal weights by ascending/descending along the mean-squared error vs filter weight curve [8] [9].

2.3.1 Method of steepest descent

The following quantities are defined for an equalizer having a real-valued input signal [8] [9].

1. Equalizer tap coefficient vector

$$f^T(k) = [\ f_0(k)\ \ f_1(k)\ \ ....\ \ f_{L_f-1}(k)\ ]$$

2. Equalizer input samples in the tapped delay line

$$r(k) = [\ r_0(k)\ \ r_1(k)\ \ ....\ \ r_{L_f-1}(k)\ ]^T$$

$$= [\ r_0(k)\ \ r_0(k-1)\ \ ....\ \ r_0(k-L_f+1)\ ]^T$$

3. Equalizer output

$$y(k) = \sum_{i=0}^{L_f-1} f_i(k) r_0(k-i) \quad = \quad f^T(k) r(k) \tag{2.11}$$

4. Error signal

$$e(k) = d(k) - y(k) \tag{2.12}$$

$$e(k) = d(k) - f^T(k)r(k) \tag{2.13}$$

where $d(k)$ is the desired signal.

The mean-squared error cost function is defined as

$$J^{MSE} = E\left\{e^2(k)\right\} \tag{2.14}$$

$$J^{MSE} = E\left\{d^2(k) - 2d(k)y(k) + y^2(k)\right\} \tag{2.15}$$

$$J^{MSE} = E\left\{d^2(k) - 2d(k)f^T(k)r(k) + f^T(k)r(k)r^T(k)f(k)\right\} \tag{2.16}$$

When the filter coefficients are fixed, the cost function can be written as

$$J^{MSE} = E\left\{d^2(k)\right\} - 2f^T E\left\{d(k)r(k)\right\} + f^T E\left\{r(k)r^T(k)\right\} f \tag{2.17}$$

$$J^{MSE} = E\left\{d^2(k)\right\} - 2f^T p + f^T R f \tag{2.18}$$

where,

$$p = E\left\{d(k)r(k)\right\} \tag{2.19}$$

which is the cross correlation vector between desired signal $d(k)$ and the equalized vector $r(k)$, while

$$R = E\left\{r(k)r^T(k)\right\} \tag{2.20}$$

which is the input signal correlation matrix.

The gradient of the MSE with respect to the equalizer tap coefficients is as follows

$$\Delta_f J^{MSE} = \frac{\partial J^{MSE}}{\partial f} = [\frac{\partial J^{MSE}}{\partial f_0} \quad \frac{\partial J^{MSE}}{\partial f_1} ..... \quad \frac{\partial J^{MSE}}{\partial L_f - 1}] \tag{2.21}$$

$$\Delta_f J^{MSE} = -2p + Rf \tag{2.22}$$

The optimum weights for (2.22) are obtained by equating the same equation to zero. Hence,

$$f = R^{-1}p \tag{2.23}$$

The method of steepest descent adjusts the tap weights in the direction of the negative gradient as follows

$$f(k+1) = f(k) + \mu\left(-\Delta_f J^{MSE}\right) \tag{2.24}$$

where, μ is the constant step size which controls the speed and accuracy of weight adaptation. For convergence, μ is chosen so as to satisfy the constraint

$$0 < \mu < \frac{1}{\lambda_{max}} \tag{2.25}$$

where, λ_{max} is the maximum eigenvalue of R.

2.3.2 Filter weight derivation for LMS algorithm

Let R and p denote the following

$$\tilde{\mathrm{R}} = r(k)r^T(k) \tag{2.26}$$

$$\tilde{\mathrm{p}} = d(k)r(k) \tag{2.27}$$

Substituting (2.26) and (2.27) into (2.22), the gradient becomes,

$$\Delta_f J^{LMS} = -2\tilde{\mathrm{p}} + 2\tilde{\mathrm{R}}f(k) \tag{2.28}$$

$$\Delta_f J^{LMS} = -2\left(d(k)r(k)\right) + 2\left(r(k)r^T(k)\right)f(k) \tag{2.29}$$

$$\Delta_f J^{LMS} = -2r(k)\left(d(k) - r^T(k)f(k)\right) \tag{2.30}$$

$$\Delta_f J^{LMS} = -2e(k)r(k) \tag{2.31}$$

Substituting the value of MSE gradient in (2.15) we obtain

$$f(k+1) = f(k) + \mu\left(-\Delta_f J^{LMS}\right) \tag{2.32}$$

$$f(k+1) = f(k) + \mu e(k)r(k) \tag{2.33}$$

where, $f(k+1)$ represents the updated filter coefficients [9].

2.3.3 Properties of LMS algorithm

In this section, some of the properties of convergence of LMS algorithm are discussed. In this study, focus is on the importance of step size μ in the convergence of the algorithm [8] [9].

2.3.3.1 Gradient behavior

The gradient of the MSE with respect to equalizer tap coefficients is as follows

$$\Delta_f J^{MSE} = 2\left[Rf - p\right]. \tag{2.34}$$

In the LMS algorithm, the instantaneous estimates of R and p are used to determine the direction. The gradient obtained by substituting these estimates is given as follows

$$\Delta_f J^{LMS} = -2\left(d(k)r(k)\right) + 2\left(r(k)r^T(k)\right) f(k) \tag{2.35}$$

Unbiased Estimate

$$E\left[\Delta_f J^{LMS}\right] = -2E\left[d(k)r(k)\right] + 2E\left[r(k)r^T(k)\right] f(k) \tag{2.36}$$

$$\Rightarrow \quad E\left[\Delta_f J^{LMS}\right] = \Delta_f J^{MSE} \tag{2.37}$$

Hence, the vector $\Delta_f J^{LMS}$ can be interpreted as an unbiased instantaneous estimate of $\Delta_f J^{MSE}$.

2.3.3.2 Convergence behavior of coefficient vector

Assume that an unknown FIR filter with coefficient vector given by f_0 is being identified by an adaptive FIR filter of the same order, employing the LMS algorithm. Measurement white noise $n(k)$ with zero-mean and variance σ_n^2 is added to the output of the unknown system. The error in the adaptive filter coefficients, as related to the ideal coefficient vector f_0, in each iteration, is described by

$$\Delta f(k+1) = \Delta f(k) + 2\mu e(k)r(k) \tag{2.38}$$

$$\Delta f(k+1) = \Delta f(k) + 2\mu r(k)\left[r^T(k)f_0 + n(k) - r^T(k)f(k)\right] \tag{2.39}$$

$$= \left[I - 2\mu r(k)r^T(k)\right]\Delta f(k) + 2\mu e_0(k)r(k) \tag{2.40}$$

where $e_0(k)$ is the optimum minimum output error, that is

$$e_0(k) = d(k) - f_0^T r(k) \tag{2.41}$$

$$e_0(k) = f_0^T r(k) + n(k) - f_0^T r(k) \tag{2.42}$$

$$e_0(k) = n(k). \tag{2.43}$$

The expected error in the coefficient vector is then given by

$$E\left[\Delta f(k+1)\right] = E\left[\left[I - 2\mu r(k)r^T(k)\right]\right]\Delta f(k) + 2\mu E\left[e_0(k)r(k)\right]. \tag{2.44}$$

If it is assumed that the elements of $r(k)$ are statistically independent of the elements of $\Delta f(k)$ and $e_0(k)$, (2.44) can be simplified as follows

$$E\left[\Delta f(k+1)\right] = (I - 2\mu R)\,E\left[\Delta f(k)\right]. \tag{2.45}$$

The assumption is that error signal at the optimal solution is orthogonal to the elements of the input signal vector. now, (2.45) simplifies to

$$E\left[\Delta f(k+1)\right] = (I - 2\mu R)^{(k+1)}\,E\left[\Delta f(0)\right]. \tag{2.46}$$

Equation (2.46) pre-multiplied by Q^T, where Q is the unitary matrix that diagonalizes R through a similarity transformation, yields

$$E\left[Q^T\Delta f(k+1)\right] = \left(I - 2\mu Q^T RQ\right)^{(k+1)}E\left[Q^T\Delta f(0)\right] \tag{2.47}$$

$$= E\left[\Delta f^{'}(k+1)\right] \tag{2.48}$$

$$= (I - 2\mu\Lambda)E\left[\Delta f^{'}(k)\right] \tag{2.49}$$

$$= \begin{bmatrix} 1-2\mu\lambda_0 & 0 & ... & 0 \\ 0 & 1-2\mu\lambda_1 & ... & 0 \\ . & . & . & . \\ . & . & . & . \\ 0 & 0 & 0 & 1-2\mu\lambda_N \end{bmatrix} E\left[\Delta f^{'}(k)\right]$$

where, $\Delta f^{'}(k+1) = Q^T \Delta f(k+1)$ is the rotated coefficient error vector. Alternatively, the above equation can be written as

$$E\left[\Delta f^{'}(k+1)\right] = (I - 2\mu\Lambda)^{(k+1)} E\left[\Delta f^{'}(0)\right] \tag{2.50}$$

$$= \begin{bmatrix} (1-2\mu\lambda_0)^{k+1} & 0 & ... & 0 \\ 0 & (1-2\mu\lambda_1)^{k+1} & ... & 0 \\ . & . & . & . \\ . & . & . & . \\ 0 & 0 & 0 & (1-2\mu\lambda_N)^{k+1} \end{bmatrix} E\left[\Delta f^{'}(0)\right]$$

This equation shows that in order to guarantee convergence of the coefficients in the mean, the convergence factor of the LMS algorithm must be chosen in the range

$$0 \;<\; \mu \;<\; \frac{1}{\lambda_{max}} \tag{2.51}$$

where λ_{max} is the largest eigenvalue of R. Values of μ in this range guarantees that all elements of the diagonal matrix in (2.50) tend to zero as $k \to \infty$, since $-1 < (1 - 2\mu\lambda_i) < 1, \quad for \quad i = 0, 1, ..., N$. As a result $E\left[\Delta f^{'}(k+1)\right]$ tends to zero for large k.

The choice of μ as above explained ensures that the mean value of the coefficient vector approaches the optimum coefficient vector. It should be mentioned that if the matrix R has a large eigenvalue spread, it is advisable to choose a value for μ much smaller than the upper bound. As a result, the convergence speed of the coefficients will be primarily dependent on the value of the smallest eigenvalue, responsible for the slowest mode in (2.50) [8] [9].

Chapter 3

Literature survey

The two major points of the research presented in this thesis are DWT-based channel estimation and DWT-based adaptive channel equalization. A survey of published literature on these topics is presented in this chapter.

3.1 Wavelet analysis

Wavelet analysis allows for a time-domain windowing technique on non-stationary signals with variable sized windows. A wavelet is a waveform of effectively limited duration that has an average value of zero. Unlike sinusoids, which are smooth, predictable and extend from minus infinity to plus infinity; wavelets are irregular, asymmetric and of limited duration. Wavelet analysis involves the use of waveform in shifted and scaled versions of the original (or mother) wavelet. The term wavelet means a small wave. The smallness refers to the condition that this window function is of finite length. The term mother implies that functions with different regions of support are derived from one main function i.e., the mother wavelet. In other words mother wavelet is a prototype for the generation other window functions. With the use of windows of wide width, low-frequency components of a signal can be analyzed, and with narrow windows high-frequency spectral components can be analyzed [5] [6].

3.2 Wavelet background

This section provides an insight that is necessary to understand and use wavelets. Wavelets possess essential properties such as compact support, vanishing moments and

dilating relation and other preferred properties such as smoothness and being a generator of an orthonormal basis of function spaces $L^2(R^n)$ etc. Compact support guarantees localization of wavelets; vanishing moments guarantees wavelet processing can distinguish the essential and non-essential information; and the dilation relation aids for fast wavelet processing algorithms [10].

3.2.1 Basics of Wavelets

The term wavelet means a small wave where smallness refers to the condition that we desire that the function is of finite length and compactly supported; and the term wave refers that the function is oscillatory.

Mother wavelet is a function $\psi(x)$ such that $\left\{\psi(2^j x - k), i, k \in Z\right\}$ is an orthogonal basis of $L^2(R)$. The basis functions are known as wavelets [10].

Dilation Equation

Let us consider a function $\phi(x)$ made up of smaller versions of itself. This is the 2-scale, dilation equation

$$\phi(x) = \sum_{k=-\infty}^{\infty} a_k \phi(2x - k). \tag{3.1}$$

In (3.1), a_k's are called the filter coefficients and the function $\phi(x)$ is called *scaling function* or father wavelet. Under specific conditions like stability, convergence, orthogonality of wavelets and scaling functions

$$\psi(x) = \sum_{k=-\infty}^{\infty} (-1)^k b_k \phi(2x - k) = \sum_{k=-\infty}^{\infty} (-1)^k \tilde{a}_{1-k} \phi(2x - k) \tag{3.2}$$

where, $\phi(x)$ is a wavelet.

Stability

The scaling function is chosen to preserve its area under each iteration, so $\sum_{-\infty}^{\infty} \phi(x) = 1$. Integrating the dilation equation in (3.1) gives

$$\sum_{-\infty}^{\infty} \phi(x)dx = \sum_{-\infty}^{\infty} a_k \phi(2x-k)dx = \frac{1}{2}\sum_{-\infty}^{\infty} a_k \phi(u)du. \tag{3.3}$$

Hence, $\sum a_K = 2$. Therefore the stability of the iteration forces a condition on a_k.

Convergence

The convergence of the wavelet expansion requires the condition $\sum_{k=0}^{N-1} (-1)^k k^m a_k = 0 \;\; where \;\; m = 0, 1, 2, ..., \frac{1}{2} - 1$.

Orthogonality of wavelets

The orthogonality of the wavelets forces the condition $\sum_{k=0}^{N-1} a_k a_{k+2m} = 0 \;\; where \;\; m = 0, 1, ...\frac{1}{2} - 1$.

Orthogonality of scaling function

The scaling function is required to be orthogonal, i.e., $\sum_{k=0}^{N-1} a_k^2 = 2$.

3.2.2 Haar and Daubechies wavelets

Let us consider the above conditions on a_k for N=2.

The stability condition implies,

$$a_0 + a_1 = 2. \tag{3.4}$$

Similarly, the accuracy constraint defines,

$$a_0 - a_1 = 0. \tag{3.5}$$

Finally, orthogonality condition gives,

$$a_0^2 + a_1^2 = 2. \tag{3.6}$$

The unique solution for the (3.4), (3.5) and (3.6) is $a_0 = a_1 = 1$. For these values of a_k,

$$\phi(x) = \phi(2x) + \phi(2x-1). \tag{3.7}$$

The refinement function is satisfied by the Box function given as

$$B(x) = \begin{cases} 1, & 0 \leq x < 1 \\ 0, & \text{otherwise} \end{cases} \tag{3.8}$$

Once the Box function is chosen as the scaling function, we obtain the Haar wavelet, as shown in Figure 3.1

$$H(x) = \begin{cases} 1, & 0 \leq x < \frac{1}{2} \\ -1, & \frac{1}{2} \leq x \leq 1 \\ 0, & \text{otherwise} \end{cases} \tag{3.9}$$

Haar wavelet represents one of the Daubechies wavelets with support at [0,1], called *db1* [10].

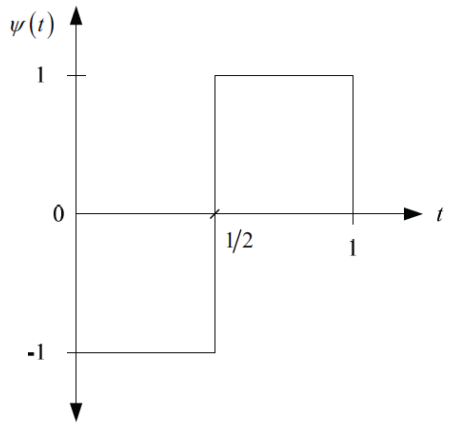

Figure 3.1 Haar wavelet.

Now considering the case for N=4, the filter coefficients become

$$a_0 + a_1 + a_2 + a_3 = 2 \tag{3.10}$$

$$a_0 - a_1 + a_2 - a_3 = 0 \tag{3.11}$$

$$-a_1 + 2a_2 - 3a_3 = 0 \tag{3.12}$$

$$a_0 a_2 + a_1 a_3 = 2 \tag{3.13}$$

$$a_0^2 + a_1^2 + a_2^2 + a_3^2 = 2 \tag{3.14}$$

The solutions are $a_0 = \frac{1+\sqrt{(3)}}{4}$, $a_1 = \frac{3+\sqrt{(3)}}{4}$, $a_2 = \frac{3-\sqrt{(3)}}{4}$, $a_3 = \frac{1-\sqrt{(3)}}{4}$. The corresponding wavelet is called Daubechies-2 (*db2*) wavelet that is supported in [0, 3] [10].

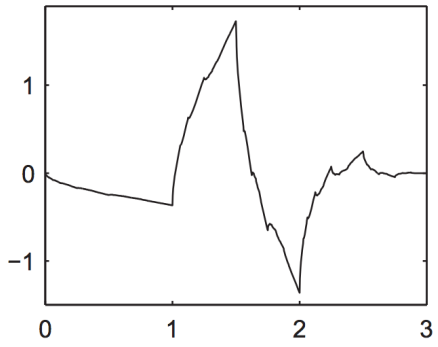

Figure 3.2 db2 wavelet.

In general, 1. the support for db_n, is on the interval [0, $2n$-1], 2. the wavelet db_n has n vanishing moments.

3.3 Discrete Wavelet Transform

The Discrete Wavelet Transform (DWT) is any transformation applied in wavelet domain for which the wavelets are sampled discretely. The DWT of a signal is calculated by decomposing the input signal simultaneously using a low pass filter of impulse response h and a high pass filter with impulse response g. These two filters are called

Quadrature Mirror Filters. The Detail coefficients are the outputs from the high pass filter, and the Approximation coefficients are the output from low pass filter. Half of the samples can now be removed, because, however half of the frequencies in the signal have been discarded through filtering[1] [11].

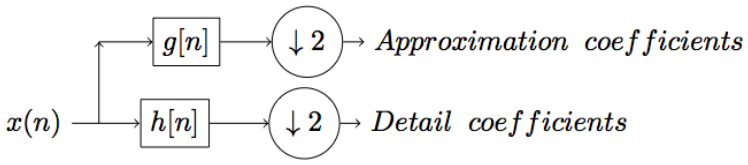

Figure 3.3 Filter analysis block diagram [1].

The Approximation and Detail coefficients in Figure 3.3 can be mathematically expressed as shown in (3.15) and (3.16)

$$y_{\mathbf{low}}[n] = \sum_{k=-\infty}^{k=+\infty} x[k]h[2n-k] \tag{3.15}$$

$$y_{\mathbf{high}}[n] = \sum_{k=-\infty}^{k=+\infty} x[k]g[2n-k]. \tag{3.16}$$

The original function $x(t)$ can be expressed in terms of wavelets in terms of an infinite summation according to

$$x(t) = \sum_{k=-\infty}^{k=+\infty} \sum_{k=-\infty}^{+\infty} d_{k.n}\psi_{k,n}(t) \tag{3.17}$$

where

$$\psi_{k,n}(t) = 2^{-n/2}\psi(2^{-n}t - k) \tag{3.18}$$

n is the dilation parameter and k is the translation parameter. The wavelets are orthonormal, i.e.,

$$\int \psi_{j,k}(t)\psi_{n,i}(t)dt = \delta_{j,n}\delta_{k,i} \tag{3.19}$$

where, $\delta_{j,n}$ and $\delta_{k,i}$ are Kronecker delta functions.

The Detail coefficients are defined as the inner product of signal and the wavelet [1],i.e,

$$d_{k,n} = \int x(t)\psi_{n,k}(t)dt \tag{3.20}$$

$$\Rightarrow d_{k,n} = \langle x, \psi_{n,k} \rangle \tag{3.21}$$

The scaling function is orthogonal to its own translations and the scaling functions are orthogonal to the wavelets for any dilation and translation [1], i.e,

$$\int \phi_{j,k}(t)\phi_{j,n}(t)dt = \delta_{k,n}, \tag{3.22}$$

$$\int \phi_{j,k}(t)\psi_{i,n}(t)dt = 0 \quad \forall i \leq j \tag{3.23}$$

The Approximation coefficients are defined as the inner product of signal and the scaling function [1], as

$$c_{k,n} = \int x(t)\phi_{k,n}(t)dt \tag{3.24}$$

$$\Rightarrow c_{k,n} = \langle x, \phi_{n,k} \rangle \tag{3.25}$$

From (3.19), (3.22) and (3.23), it can be inferred that

$$\{\phi(t-k); \psi(t-k)\}_{k=-\infty}^{k=+\infty} \tag{3.26}$$

is a set of orthonormal basis. Similarly, from the previous section, from the dilation equation (3.1) we have that

$$\sqrt{2}\left\{\phi(2t-k)\right\}_{k=-\infty}^{k=+\infty} \tag{3.27}$$

are also an orthonormal basis set. Hence, any function $p(t)$ can be expanded as

$$p(t) = \sum_{k} a^0(k)\sqrt{2}\phi(2t-k) \tag{3.28}$$

where, $a_0(k)$ are the coefficients used to represent $p(t)$ with $\phi(2t-k)$.

It can also be written using two orthonormal basis as

$$p(t) = \sum_{k}[a^1(k)\sqrt{2}\phi(t-k) + b^1(k)\sqrt{2}\psi(t-k)] \tag{3.29}$$

where, $a^j(k)$ and $b^j(k)$ are the weighting functions used for the scaling function and the mother wavelet at j^{th} level of resolution [1].

Again, using the dilation equation for the scaling function (3.1)

$$\phi(t-n) = \sqrt{2}\sum_{k} \tilde{\mathrm{h}}(k)\phi(2t-2n-k) \tag{3.30}$$

Similarly, the mother wavelet can be expressed as

$$\psi(t-n) = \sqrt{2}\sum_{k} \tilde{\mathrm{g}}(k)\phi(2t-2n-k) \tag{3.31}$$

$a^1(n)$ are used to express $p(t)$ with $\phi(t-n)$ as

$$a^1(n) = \int_{-\infty}^{+\infty} p(t)\phi(t-n)dt \tag{3.32}$$

$$\Rightarrow \quad a^1(n) = \int_{-\infty}^{+\infty} p(t)\sqrt{2}\sum_k \tilde{\mathrm{h}}(k)\phi(2t-2n-k)dt \tag{3.33}$$

$$\Rightarrow \quad a^1(n) = \sum_k \tilde{\mathrm{h}}(k)a^0(2n+k) \tag{3.34}$$

$$\Rightarrow \quad a^1(n) = \sum_k a^0(k)\tilde{\mathrm{h}}(k-2n) \tag{3.35}$$

similarly,

$$\Rightarrow \quad b^1(n) = \sum_k a^0(k)\tilde{\mathrm{g}}(k-2n) \tag{3.36}$$

A bijective mapping can now be formed between $a^1(n)$ and $b^1(n)$, as well as Approximation and Detail coefficients, respectively, as follows [1]:

$$c_{k,j} \leftrightarrow a^j(k) \tag{3.37}$$

and

$$d_{k,j} \leftrightarrow b^j(k). \tag{3.38}$$

Hence, (3.37) and (3.38) can be generalized as

$$c_{k,j+1} = \sum_n c_{n,j}\tilde{\mathrm{h}}(n-2k) \tag{3.39}$$

$$\Rightarrow \quad \sum_n c_{n,j}h(N+2k-n) \quad \forall j \geq 0 \tag{3.40}$$

and

$$d_{k,j+1} = \sum_n c_{n,j}\tilde{\mathrm{g}}(n-2k) \tag{3.41}$$

$$\Rightarrow \quad \sum_{n} d_{n,j} g(N + 2k - n) \quad \forall j \geq 0. \tag{3.42}$$

The above equations (3.39) to (3.42) explain the method of performing DWT and obtaining the Detail and Approximation coefficients recursively. The important point of notice is that, there is no need to explicitly know the scaling function and mother wavelet for computing the DWT; instead the **Perfect Reconstruction filters** h(n), g(n), $\tilde{\mathrm{g}}(n)$ and $\tilde{\mathrm{h}}(n)$ are sufficient[1] [12].

Even though the DWT is expressed as an infinite sum, in practical situations, it is expressed as a finite sum as follows

$$x(t) = \sum_{n=0}^{M} \sum_{k} d_{k.n} \psi_{k,n}(t) + \sum_{k} c_{k,M} \phi_{M,k}(t) \tag{3.43}$$

From (3.43) we see that, $x(t)$ is expressed predominantly in terms of Detail coefficients till a resolution of M, but at a level of resolution of $n = M$, it is expressed as a combination of Detail and Approximation coefficients.

3.4 Discrete Wavelet Transform-based Channel Estimation

Wavelets have been used in the identification of time-varying system/channel models. This identification is made possible, if each time-varying system coefficient are expanded onto a finite set of basis sequences [13]. Wavelets find their application as basis sequences as they are better flexible in capturing the signal characteristics at different scales.

In the survey of channel estimation methods, first a system model with known input and output functions are considered. Then the unknown channel impulse response is expanded onto a set a predefined basis function which are wavelets. A Least Squares (LS) method is applied to obtain the correlation matrix of the expansion coefficients. A subspace method is employed to recover the expansion coefficients from the correlation matrix from which the system impulse response is estimated [14].

In another study, a Wavelet-based blind maximum likelihood sequence estimator is proposed [15]. The channel is represented in a reduced order dimensional space by matching the scattering function of the multipath channel to its decomposition and obtain an approach to per survivor processing. These processing techniques are effective in fast fading environments like those found in macro cell communication systems [15]. Using such a Wavelet-based representation of the channel, generalized likelihood detection statistics for TDMA [15] and DS/CDMA [16] signals are devised.

In [17], the multiplicative channel fading effect is modelled as an auto regressive process. The transmitted signals are precoded using filter banks and the second-order statistics of the output are computed which gives the correlation information of the time-varying channel. Next, a Kalman filter is used to track the changes in the time-varying channel and recover the transmitted signals in a block-by-block fashion.

In another survey of wavelets used for estimation, a semi-blind joint channel estimation and data detection algorithm based on the EM algorithm that integrates the advantages of Wavelet-based parameter estimation is proposed [18]. This focuses on reducing the number of estimated parameters by iteratively discarding insignificant wavelet coefficients from the estimation process. This algorithm outperforms pilot-based channel estimation techniques and other semi-blind channel estimation schemes in terms of complexity, bit error rate, and mean square error.

In [19], Maximum Likelihood (ML) data-aided channel estimation for wavelet packets based ultra wideband (WP-UWB) transmissions is devised. An optimum training sequences criterion is derived. Based on this, nearly optimum perfect root of unity sequences (PRUS) are tested and compared to Gold sequences and random sequences. In this estimation strategy, a generalized inverse of the training pilot symbols matrix can be pre-computed and stored in memory. This technique is especially attractive for low data rate transmissions as in sensor networks because of its low complexity implementation.

In another set of studies, the main problem in underwater acoustics, i.e., identification of underwater channel is solved by employing wavelet packet analysis. This wavelet

packet analysis provides good results, by improving the temporal resolution of acoustic signals [20].

3.5 Discrete Wavelet Transform-based Adaptive Equalization

In the context of communications systems, in addition to the estimation of channel impulse responses, an equalization procedure shall be developed in the receiver to combat the effects of ISI. A linear Equalizer can be employed in this case if the channel distortion is optimal, and a Decision Feedback Equalizer is employed if the distortion is severe. But in both the cases the convergence rate is slow. Hence, in [21], a Wavelet-based Linear Equalizer (WBLE) and Wavelet-based Decision Feedback Equalizer are developed. The work shows that Wavelet-based equalization methods have better performance as they converge faster than their counter parts. Also, the choice of wavelets has an insignificant effect on the performance.

In other works [22], [23] various adaptive equalization methods including the Least Mean Squares (LMS) Equalizer, Recursive Least Squares (RLS) Equalizer and Wavelet transform domain equalizer are studied. The LMS method minimizes the Mean Square Error (MSE) between the equalized output and the transmitted input sequence in each iteration. RLS equalizer performs better than LMS equalizer as the convergence rate is higher. But it has the disadvantage of higher complexity. The Discrete Wavelet Transform Adaptive Equalizer performs better than the other two in terms of mean square error and computational complexity.

In [1], the Zero Forcing Equalizer (ZFE) and Minimum Mean Square Error Equalizer (MMSE) are developed in the discrete wavelet transform domain. A pilot-assisted wavelet-domain channel equalization has been established, specifically by making use of the techniques of wavelet-domain convolution. It has also been shown that signals propagating through a fast fading channel are equalized with approximately the same performance in the wavelet-domain and the time-domain.

In [24], an orthonormal Wavelet-based equalizer (OWBE) was developed. The equalizer is represented by wavelets with corresponding coefficients. Theoretical analysis and experimental results show that the input correlation matrix, after an orthonormal transform, is almost diagonalized, thus converges faster, even in case of a large eigenvalue spread. In addition, the wavelets have good time-frequency localization, so that the OWBE is applicable even in case of time-variant channels.

Wavelet filter banks have also found their applications in the design of an equalizer [25]. This approach is known to improve the convergence rate of blind equalizers and to decrease their computational cost. This method mainly deals with the cyclo-stationary approach used in most fractionally spaced equalizers. Reasonable performance has been shown when the channel has considerable length, in the presence of fractional delays and non-minimum phase parts in the channel, as well as when the received data are highly correlated.

Multiresolution wavelet equalization can also be employed to combat the ISI effects of the channel, since wavelet transforms exploit the time-frequency representation. The basic idea to apply wavelets is the exploitation of the bandwidth decomposition to selectively recover the alterations introduced by the channel. It is proven that using wavelets as filters and exploiting the multiresolution decomposition of the received signal, the ISI can be significantly reduced [26].

Chapter 4

Technical preliminaries

This chapter describes the technical preliminaries required to develop a method for DWT-based channel estimation. The topics discussed in this chapter are namely, Multiresolution analysis, subband coding, and a method for convolution in wavelet domain.

4.1 Mutiresolution analysis and subband coding

Multiresolution Analysis (MRA) is a technique used to analyze the signal at different frequencies with different resolutions. MRA is designed to give good time resolution and poorer frequency resolution at higher frequencies and good frequency resolution and poor time resolution at lower frequencies. This makes sense when the signal we encounter has high frequency components for short duration and low frequency components for long duration and fortunately signals in practical applications are of this type. The specific approach of MRA that is used in DWT is called subband coding [12]. In MRA, filters of different cut-off frequencies are used to analyze the signals at different scales. The signal is passed through a series of high pass filters to analyze high frequencies and it is passed through a series of low pass filters to analyze low frequencies. The resolution of the signal, which is a measure of the amount of detail information in the signal is changed by the filtering operations, and the scale is changed by either upsampling, or downsampling operations [1].

In Figure 4.1, the input signal is divided into two streams, one with low pass filter and the other with high pass filter.

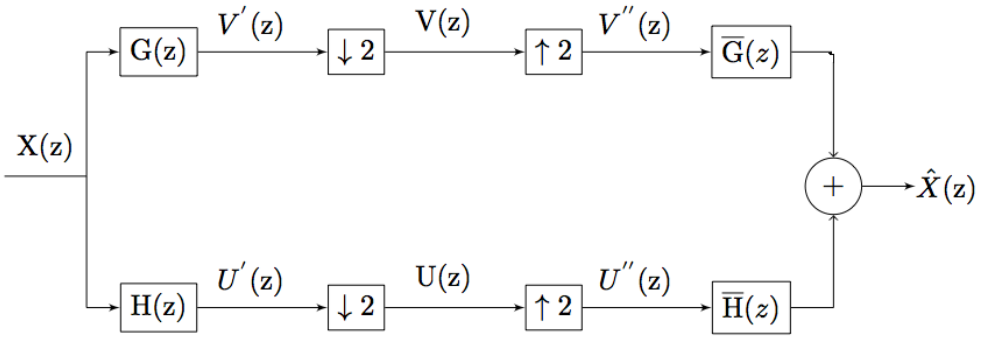

Figure 4.1 Two-channel subband coding analysis and synthesis [1].

In Figure 4.1 we have that,

$G(z)$ is the analysis high pass filter of limiting frequencies $\pi/2 \leq \omega \leq \pi$

$H(z)$ is the analysis low pass filter of limiting frequencies $0 \leq \omega \leq \pi/2$

$\overline{\mathrm{G}}(z)$ is the synthesis high pass filter

$\overline{\mathrm{H}}(z)$ is the synthesis low pass filter

Consider a discrete-time input signal, $x(n)$,which is bandlimited to π rad/sec that has the z-transform

$$X(z) = \sum_{n} x(n) z^{-n} \tag{4.1}$$

where

$$z = e^{j\omega}. \tag{4.2}$$

The intermediate signals obtained in the operation are

$$V^{'}(z) = X(z)G(z) \tag{4.3}$$

$$U^{'}(z) = X(z)H(z). \tag{4.4}$$

As shown in Figure 4.1, the signals $V^{'}(z)$ and $U^{'}(z)$ are now down sampled by a factor of 2 to obtain the following intermediate signals

$$V(z) = \frac{1}{2}[V^{'}(z^{\frac{1}{2}}) + V^{'}(-z^{\frac{1}{2}})] \tag{4.5}$$

$$U(z) = \frac{1}{2}[U^{'}(z^{\frac{1}{2}}) + U^{'}(-z^{\frac{1}{2}})]. \tag{4.6}$$

Now, the signals are up sampled by a factor of 2 as indicated below

$$V^{''}(z) = V(z^2) \tag{4.7}$$

$$U^{''}(z) = U(z^2). \tag{4.8}$$

Substituting (4.5) and (4.6) in (4.7) and (4.8) we get

$$V^{''}(z) = \frac{1}{2}[V^{'}(z) + V'(-z)] \tag{4.9}$$

$$U^{''}(z) = \frac{1}{2}[U^{'}(z) + U'(-z)]. \tag{4.10}$$

Hence, the output of the filter bank can be written as

$$\hat{\mathrm{X}}(z) = V^{''}(z)\tilde{\mathrm{G}}(z) + U^{''}(z)\tilde{\mathrm{H}}(z). \tag{4.11}$$

Substituting (4.9) and (4.10) into (4.11) we get

$$\hat{\mathrm{X}}(z) = \frac{1}{2}[V^{'}(z) + V'(-z)]\tilde{\mathrm{G}}(z) + \frac{1}{2}[U^{'}(z) + U'(-z)]\tilde{\mathrm{H}}(z)]. \tag{4.12}$$

Substituting (4.3) and (4.4) into (4.12), $\hat{\mathrm{X}}(z)$ can be expressed in terms of original signal $X(z)$ as

$$\hat{\mathrm{X}}(z) = \frac{1}{2}[X(z)G(z) + X(-z)G(-z)]\tilde{\mathrm{G}}(z)] + \frac{1}{2}[X(z)H(z) + X(-z)H(-z)]\tilde{\mathrm{H}}(z)] \quad (4.13)$$

$\Rightarrow$

$$\hat{\mathrm{X}}(z) = \frac{1}{2}[G(z)\tilde{\mathrm{G}}(z) + H(z)\tilde{\mathrm{H}}(z)]X(z) + \frac{1}{2}[G(-z)\tilde{\mathrm{G}}(-z) + H(-z)\tilde{\mathrm{H}}(-z)]X(z) \quad (4.14)$$

Hence, from the above equations it is clear that the received signal $\hat{\mathrm{X}}(z)$ contains both the transmitted signal $X(z)$ and also the alias of the transmitted signal (second term). In order for the received signal to be equal to the transmitted signal, the alias term must be zero [1]. Therefore,

$$G(-z)\tilde{\mathrm{G}}(-z) + H(-z)\tilde{\mathrm{H}}(-z) = 0 \quad (4.15)$$

Consider $H(z)$ to be a finite impulse response filter of order $N+1$ where N is always an odd number. The anti-aliasing condition in (4.15) can be satisfied by choosing

$$\tilde{\mathrm{G}}(z) = -H(z) \quad (4.16)$$

$$G(z) = \tilde{\mathrm{H}}(z). \quad (4.17)$$

Now, consider the definitions that

$$\tilde{\mathrm{H}}(z) \triangleq z^{-N}H(z^{-1}) \quad (4.18)$$

$\Rightarrow$

$$\tilde{\mathrm{h}}(n) \triangleq h(N-n) \quad (4.19)$$

and

$$\tilde{\mathrm{G}}(z) \triangleq z^{-N} G(z^{-1}) \tag{4.20}$$

$\Rightarrow$

$$\tilde{\mathrm{g}}(n) \triangleq g(N-n). \tag{4.21}$$

Now, by using these equations $G(z)$ can be written in terms of $H(z^{-1})$ as

$$G(z) = \tilde{\mathrm{H}}(-z) = (-z)^{-N} H((-z)^{-1}) \tag{4.22}$$

$\Rightarrow$

$$G(z) = -z^{-N} H(-z^{-1}) \tag{4.23}$$

since N is always odd.

Now, $\tilde{\mathrm{X}}(z)$ can be written in terms of H(z) as

$$\tilde{\mathrm{X}}(z) = \frac{1}{2}[H(-z)H(-z^{-1}) + H(z)H(z^{-1})]z^{-N}X(z). \tag{4.24}$$

The above equation implies that if the filter $H(z)$ is designed in such a way that

$$H(-z)H(-z^{-1}) + H(z)H(z^{-1}) = 2 \tag{4.25}$$

then the received estimate signal will be equal to transmitted signal with N delays. Using the mapping $z = e^{j\omega}$ in the above equation, it gives

$$|H(e^{j\omega})|^2 + |H(e^{j(\omega+\pi)}|^2 = 2. \tag{4.26}$$

The above equation is the criterion for perfect reconstruction and the filters $H(z)$ and $G(z)$ are called **Quadrature Mirror Filters (QMF)**. Hence, from these derivations

it is clear that if the filter $H(z)$ is known, the other filters can be constructed based on the Perfect Reconstruction criterion [1] [12] [27] [28] [29].

4.2 Convolution in discrete wavelet domain

Convolution is an operation performed on two signals which involves multiplying one signal with delayed and shifted versions of other, averaging and repeating the process for several delays. It is a very useful process, as it describes the effects of various scientific measurements, like effects of various filters on signals. Convolution is well defined in various domains such as Time domain, Laplace domain, Z-domain and Fourier domains. In this thesis, signal processing will be carried out in the wavelet domain, primarily using the discrete wavelet transform.

The use of convolution in the context of subband coding as discussed previously involves the use of multirate filters. The underlying concept of this approach is the merging/moving the filter that is placed at the input of DWT filter bank to the positions in the analysis sections of the filter banks. This method is termed the Forward Merge Approach. It can be extended by using polyphase filters, thereby proving an equivalent mechanism for DWT-based convolution [1].

As seen in the Figure 4.2, the filters on the left side are called the analysis filters $H_m(z)$ and the filters on the right side are called the synthesis filters $F_m(z)$. The input signal is split into M streams by the analysis filters, then down sampled by a factor of M. The resulting sequence $x_m(n)$ is up sampled back by the factor of M and then synthesized into $\tilde{\mathrm{x}}(n)$ by the synthesis filters.

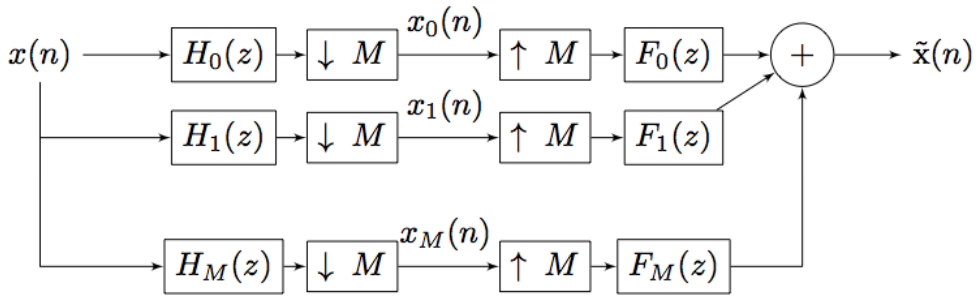

Figure 4.2 M channel Filter bank [1].

4.2.1 Noble identities of Multirate filters

Consider the following operation in Figure 4.3

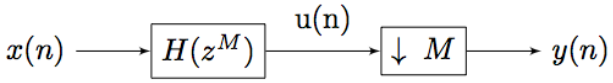

Figure 4.3 Filtering followed by downsampling [1].

As shown in the Figure 4.3, the input signal is first filtered and then decimated by a factor of M. Hence, the output of the filter will be

$$U(z) = H(z^M)X(z). \tag{4.27}$$

Secondly, the intermediate signal is now being decimated by a factor of M. Thereby the output after the decimation is as follows

$$Y(z) = \frac{1}{M}\sum_{k=0}^{M-1} U(z^{1/M})e^{-j2\pi k/M} \tag{4.28}$$

$$Y(z) = \frac{1}{M}[X(z^{1/M})H(z) + X(-z^{1/M})H(z)] \tag{4.29}$$

$$\Rightarrow Y(z) = \frac{1}{M}[X(z^{1/M} + X(-z^{1/M}]H(z). \tag{4.30}$$

The above equation (4.30) indicates that the input signal can be first decimated by a factor of M and then filtered, instead of first filtering and later decimating. This relationship is depicted in Figure 4.4.

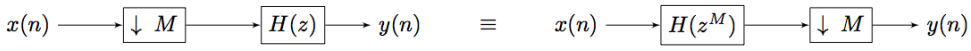

Figure 4.4 The first identity [1].

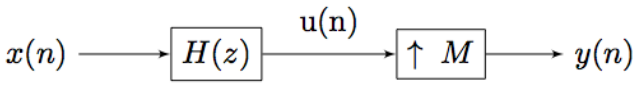

Figure 4.5 Filtering followed by upsampling [1].

Now, in the case of employing a upsampler as seen in Figure 4.5, the following equations can be derived

$$U(z) = X(z)H(z) \tag{4.31}$$

$$Y(z) = U(z^M). \tag{4.32}$$

Substituting (4.31) in (4.32) we get

$$Y(z) = X(z^M)H(z^M). \tag{4.33}$$

The above equation, (4.33) implies that the input signal, $x(n)$, may be filtered and then upsampled instead of being up sampled first and then filtered. This is shown in Figure 4.6.

Figure 4.6 The second identity [1].

4.3 Forward Merge approach

The topic of this research, namely the DWT-based convolution, involves performing convolution in the wavelet-domain unlike the convolution in time-domain. Consider the basic convolution strategy in Figure 4.7.

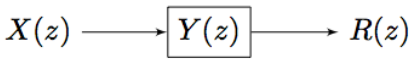

Figure 4.7 Basic Convolution.

From the Figure 4.7, the following equations can be written

$$x(n) * y(n) = r(n) \tag{4.34}$$

$$X(z)Y(z) = R(z). \tag{4.35}$$

Now, $R(z)$ can be analyzed and synthesized using analysis and synthesis filters as seen in previous section. This scenario where $R(z)$ is transformed using DWT/IDWT is depicted in Figure 4.8.

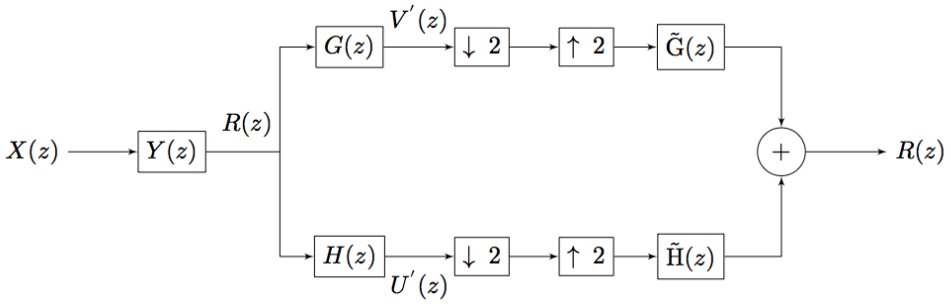

Figure 4.8 Level-1 DWT and IDWT of $R(z)$ [1].

Forward merge approach uses some of the properties discussed in the previous section and merges $Y(z)$ within the analysis/synthesis sections of $R(z)$. From Figure 4.8, the intermediate signals are as follows

$$V'(z) = R(z)G(z) \tag{4.36}$$

and

$$U^{'}(z) = R(z)H(z). \tag{4.37}$$

Using (4.35), the above equations can be simplified as follows

$$V^{'}(z) = X(z)Y(z)G(z) \tag{4.38}$$

and

$$U^{'}(z) = X(z)Y(z)H(z). \tag{4.39}$$

By using the equations (4.38) and (4.39), the Figure 4.8 can be modified as shown in Figure 4.9 by moving the convolution operation which was originally outside the DWT/IDWT filter banks to the inside. Also the order of filtering of $G(z)$ with $Y(z)$ can be interchanged as filtering is commutative. It is the same case with the order of filtering with $H(z)$ and $Y(z)$ [1].

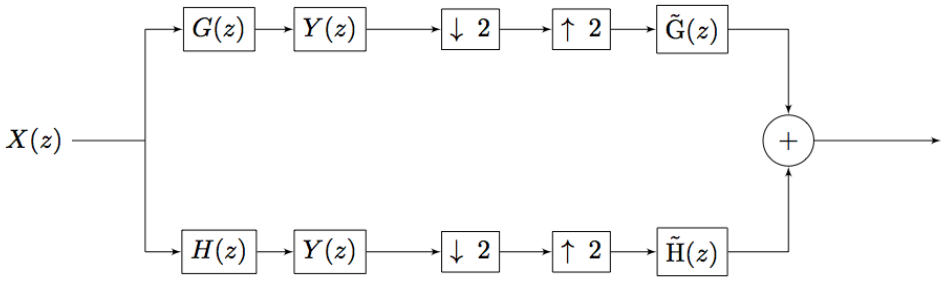

Figure 4.9 Forward merge approach of DWT convolution [1].

DWT-based convolution at level 2 is basically a level-1 DWT of the approximation coefficients at the first level of the overall DWT. This is shown in Figure 4.10.

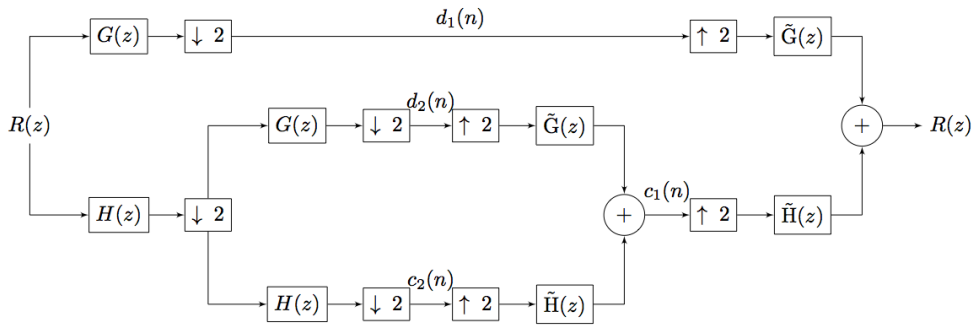

Figure 4.10 Original 2-level DWT/IDWT filter bank [1].

The original DWT/IDWT of $R(z)$ can be modified by moving the decimator following $H(z)$ in level 1 to level 2. Here, two filters namely $G(z)$ and $H(z)$ in level 2 follows decimator in level 1. Hence, the decimator can be moved into level 2 ahead of the filters $G(z)$ and $H(z)$ by applying the second noble identity discussed in the Subsection 4.2.1. This modified level-2 DWT/IDWT is illustrated in Figure 4.11.

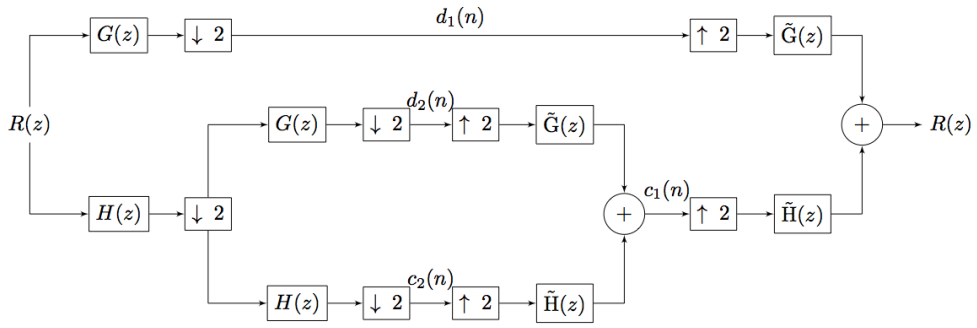

Figure 4.11 Modified 2-level DWT/IDWT filter bank [1].

The Forward Merge Approach of convolving $X(z)$ and $Y(z)$ can now be implemented by using the modified filter bank in Figure 4.11. The resulting filter bank is shown in Figure 4.12. Using the modified DWT/IDWT filter banks the Forward Merge Approach can be implemented for any number of levels of DWT analysis [1].

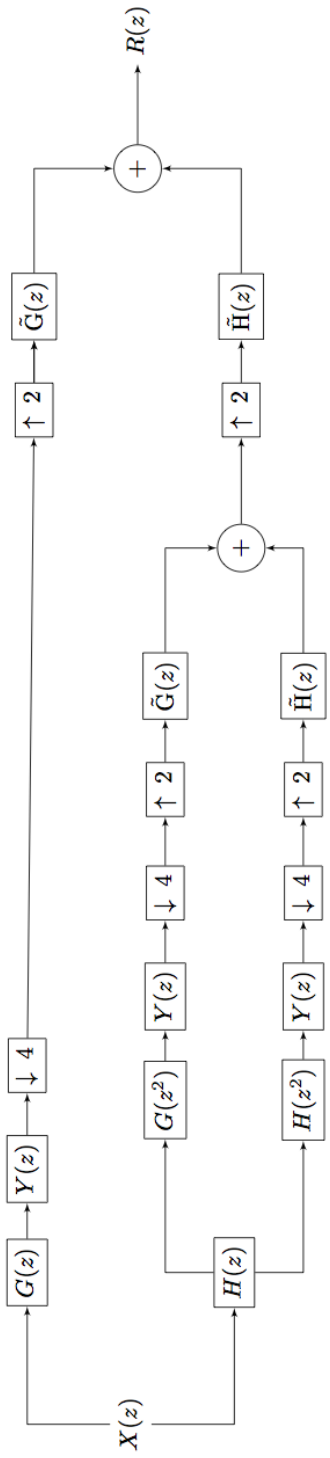

Figure 4.12 Forward Merge approach at two levels of DWT [1].

Chapter 5

DWT-based channel estimation

In DWT-based channel estimation, the channel is first estimated using a pilot signal and then the actual data-bearing signals are transmitted. A pilot signal is transmitted and a copy of the same signal is available at the receiver. Using these two signals, i.e., one corrupted and the other uncorrupted signals can be used to estimate the channel. In particular, deconvolution can be applied to estimate the channel, where the received distorted pilot is deconvolved with the available copy at the receiver.

In this chapter, a deconvolution technique for channel estimation is performed in the wavelet-domain and comparison is made with the channel estimates obtained by time-domain methods.

5.1 Deconvolution using DWT

Let $x(n)$ be an input signal (finite length discrete sequence) to be transmitted and $y(n)$ be the finite length discrete channel impulse response. Suppose $r(n)$ is the output, of the channel obtained from the convolution given by

$$r(n) = x(n) * y(n). \tag{5.1}$$

The convolution indicated in (5.1) can be performed using the Forward Merge Approach as follows where, $X(z)$ and $Y(z)$ are Z-transform equivalents of $x(n)$ and $y(n)$, respectively.

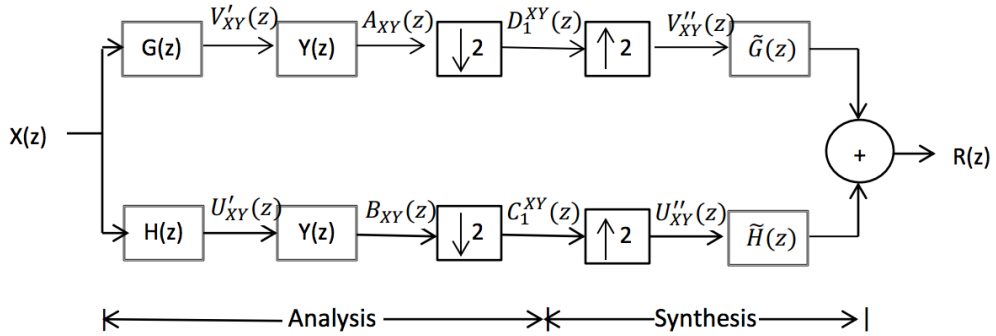

Figure 5.1 DWT convolution of $X(z)$ and $Y(z)$ [1].

Here $D_1^{XY}(z)$ and $C_1^{XY}(z)$ are the z-transforms of the Detail and Approximation coefficients, respectively. Specifically,

$$D_1^{XY}(z) = \sum_{n=0}^{L_{d_1}} d_1(n) z^{-n} \tag{5.2}$$

$$C_1^{XY}(z) = \sum_{n=0}^{L_{c_1}} c_1(n) z^{-n} \tag{5.3}$$

where L_{d_1} and L_{c_1} are the lengths of $d_1(n)$ and $c_1(n)$, respectively.

In the synthesis part of the above diagram, the Detail and Approximation coefficients $D_1^{XY}(z)$ and $C_1^{XY}(z)$ are up-sampled by a factor of 2 which results in

$$V''_{XY}(z) = D_1^{XY}(z^2) \tag{5.4}$$

$$U''_{XY}(z) = C_1^{XY}(z^2). \tag{5.5}$$

The signals are then filtered to produce the convolved output, i.e.,

$$R(z) = V''_{XY}(z)\tilde{\mathrm{G}}(z) + U''_{XY}(z)\tilde{\mathrm{H}}(z) \tag{5.6}$$

using equations (5.4) and (5.5), the above equation can be expressed as

$$R(z) = D_1^{XY}(z^2)\tilde{\mathrm{G}}(z) + C_1^{XY}(z^2)\tilde{\mathrm{H}}(z) \tag{5.7}$$

The convolution of $X(z)$ and $Y(z)$ can be analyzed and synthesized with DWT/IDWT filter banks as follows

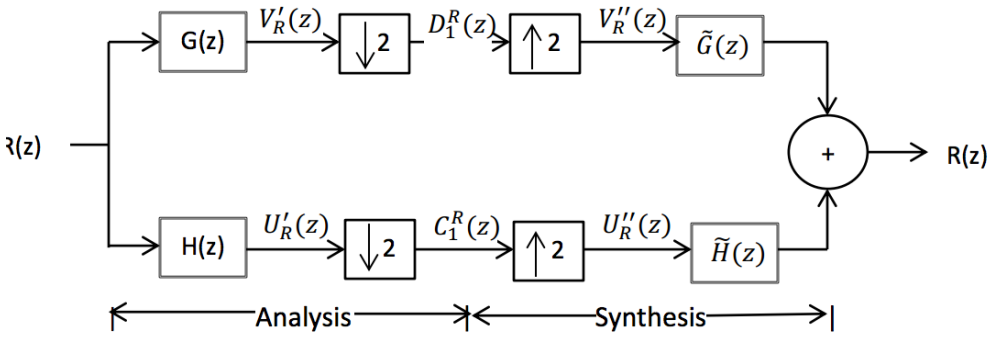

Figure 5.2 DWT and IDWT of $R(z)$ [1].

Here $R(z)$ can be expressed in terms of the Detail and Approximation coefficients $D_1^R(z)$ and $C_1^R(z)$ as follows

$$R(z) = D_1^R(z^2)\tilde{\mathrm{G}}(z) + C_1^R(z^2)\tilde{\mathrm{H}}(z). \tag{5.8}$$

As seen from (5.7), $R(z)$ can be expressed in terms of the Detail and Approximation coefficients of the convolution of $X(z)$ and $Y(z)$. And from (5.8) $R(z)$ is expressed in terms of its own Detail and approximation coefficients. Hence, by comparing the (5.7) and (5.8), the following can be observed.

$$D_1^{XY}(z^2) = D_1^R(z^2) \tag{5.9}$$

$$C_1^{XY}(z^2) = C_1^R(z^2) \tag{5.10}$$

This implies,

$$D_1^{XY}(z) = D_1^R(z) \tag{5.11}$$

$$C_1^{XY}(z) = C_1^R(z) \tag{5.12}$$

The DWT Detail and Approximation coefficients in Figure 5.1 can be expressed in terms of intermediate coefficients as follows

$$D_1^{XY}(z) = \frac{1}{2}[A_{XY}(z^{1/2}) + A_{XY}(-z^{1/2})] \tag{5.13}$$

$$C_1^{XY}(z) = \frac{1}{2}[B_{XY}(z^{1/2}) + B_{XY}(-z^{1/2})]. \tag{5.14}$$

Similarly, from Figure 5.2, the DWT Detail and Approximation coefficients of $R(z)$ can be also expressed in terms of intermediates as follows

$$D_1^{R}(z) = \frac{1}{2}[V_R^{'}(z^{1/2}) + V_R^{'}(-z^{1/2})] \tag{5.15}$$

$$C_1^{R}(z) = \frac{1}{2}[U_R^{'}(z^{1/2}) + U_R^{'}(-z^{1/2})]. \tag{5.16}$$

Hence, from the (5.11) through (5.16), it can be concluded that

$$A_{XY}(z) = V_R^{'}(z) \tag{5.17}$$

$$B_{XY}(z) = U_R^{'}(z). \tag{5.18}$$

From Figure 5.1, we note that

$$A_{XY}(z) = V_{XY}^{'}(z)Y(z) \tag{5.19}$$

$$B_{XY}(z) = U_{XY}^{'}(z)Y(z). \tag{5.20}$$

Using the results of (5.17) and (5.18) in (5.19) and (5.20) we get

$$V_R^{'}(z) = V_{XY}^{'}(z)Y(z) \tag{5.21}$$

$$U_R^{'}(z) = U_{XY}^{'}(z)Y(z). \tag{5.22}$$

Expressing $V_{XY}^{'}(z)$ and $U_{XY}^{'}(z)$ as inverses, Y(z) can be expressed as

$$Y(z) = V_{XY}^{-1}(z)V_R^{'}(z) \tag{5.23}$$

$$Y(z) = U_{XY}^{-1}(z)U_R'(z) \tag{5.24}$$

The equations (5.23) and (5.24), show that the channel estimates, $Y(z)$ can be calculated by directly deconvolving the DWT coefficients obtained through the convolution of $X(z)$ and $Y(z)$ from the DWT coefficients of $R(z)$. In one case this uses the Detail coefficients, and in the other case the Approximation coefficients are used [1].

5.2 Computer simulation experiments

The deconvolution procedure using the DWT can be verified by performing computer simulation experiments. The two important phases of a simulation experiment are:

1. Test Signal Generation

2. Channel Impulse Response Generation

Each test signal is composed of sum of odd harmonics of fundamental sinusoidal component. The general form of the signal in discrete time is

$$S(n) = \sum_{k=1}^{K} A_k cos[(2k-1)2\pi f_0 n T_s + \phi_k] \tag{5.25}$$

where, $S(n)$ is the $n'th$ element of the test signal sequence,

K is the number of sinusoidal harmonic components in the test signal,

A_k is the amplitude of the $k'th$ harmonic component,

f_0 is the frequency of the fundamental harmonic,

T_s is the sampling rate, and

Φ_k is the additional phase offset for the $k'th$ harmonic.

The values of amplitudes and phase are obtained from a pdf that has a the Uniform distribution describing each parameter. The Amplitude is Uniformly distributed between 0 and 10. Similarly, the Phase offsets are Uniformly distributed between 0 to

2π radians. The frequency of the fundamental harmonic f_0 is fixed at a value of 2kHz and the number of odd harmonics K is fixed at the value of 7. Two different channel models are considered in the experiments:

1. Gaussian PDP channel.

2. Exponential PDP channel.

In practice channels are not, typically characterized by a time-domain impulse response in either analytical or empirical models based on measurements. Instead, the power delay profile of a channel is established, either as an analytical model or empirically by channel sounding measurements.

5.2.1 Experimental procedure

Simulation experiments are performed for the following scenarios:

1. Two channel PDP models.

2. Two cases of fading per channel.

3. Addition of white Gaussian noise to every transmitted signal.

4. Use of Haar, db2, db3, and db4 wavelets in the channel estimation algorithm.

In each experiment, the test signal is convolved with the channel impulse response and an additive white Gaussian noise with a double-sided Power Spectral Density (PSD) of $\frac{N_0}{2}$ is added to signal appearing at the output.

Each received signal is analyzed to four levels of DWT resolution. Hence, there are five estimates i.e., four estimates of detail coefficients obtained at each of four levels of resolution and an estimate obtained from the approximation coefficient at the fourth level of resolution. The parameter $\frac{E_b}{N_0}$ is used throughout this work to provide a relative measure of the energy contained in every information bit that is transmitted.

In each experiment the Mean Square Error (MSE) between the actual channel impulse response and the estimated channel impulse response is computed. A total of 1000 test

signals are transmitted for each value of $\frac{E_b}{N_0}$. An average of the resulting ensemble of 1,001 MSEs for each value of $\frac{E_b}{N_0}$ is then computed.

5.3 Results

For each channel PDP, two fading scenarios are considered, one is Fast fading and the other is Slow fading. This is differentiated by selecting a suitable value of normalized delay time d. The value of d is 0.2 for a fast fading channel and it is 2.5 for a slow fading channel.

Let τ denote the Root-Mean-Squared (RMS) delay spread, and is defined by

$$\tau = dT_{sym} \tag{5.26}$$

T_{sym} is the period of baseband digital symbols. It is set to 1 sec in all experiments.

5.3.1 Channel 1: Gaussian power delay profile

The Gaussian PDP is defined as

$$\phi_c(t) = 1/(\sqrt{2\pi\tau})exp\frac{-(t/\tau)^2}{2}. \tag{5.27}$$

The duration of $\phi_c(t)$ is fixed at 5 sec for all simulations using this Gaussian PDP channel. The baseband symbol period for the test signal is 1 sec, and the test signal is composed of 10 symbols. Furthermore, each symbol period is sampled at a rate of 10 samples/symbol. Due to this condition the test signal is composed of 100 sample values, and the channel impulse response is composed of 50 sample values. The two PDP's corresponding to fast fading and slow fading in a Gaussian PDP channel are shown in Figure 5.3 and Figure 5.4.

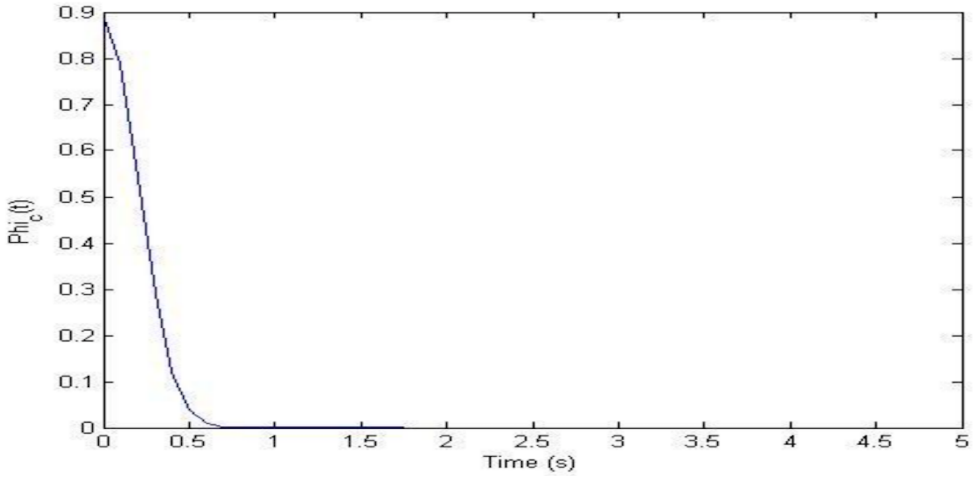

Figure 5.3 Gaussian PDP for fast fading.

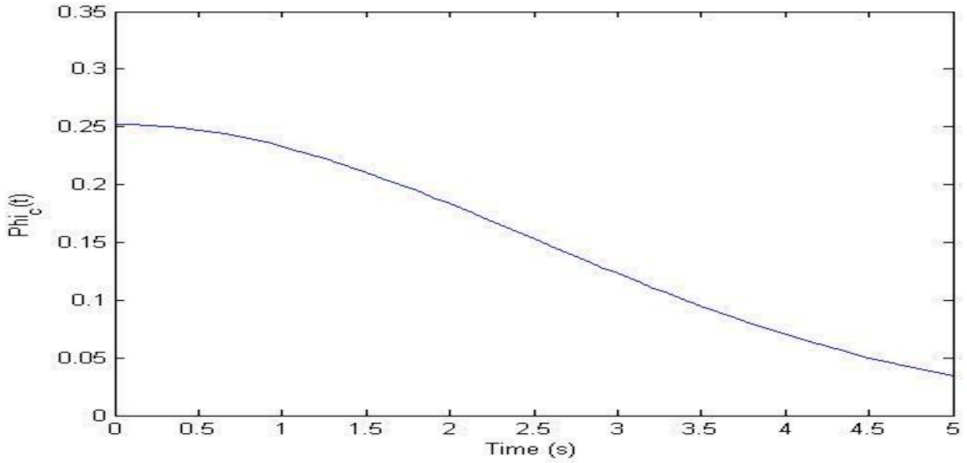

Figure 5.4 Gaussian PDP for slow fading.

The Figures 5.5-5.8 illustrated plots of MSE's for various values of $\frac{E_b}{N_0}$ in a Gaussian PDP case. The MSE's between the four detail coefficient estimates, one approximation based estimate at the fourth level of resolution and the actual channel impulse responses are plotted using various colored lines in each figure. The estimate of the impulse response using time-domain deconvolution is also plotted in the figures. As seen in this case, the performance of channel estimation using the Level 1 Detail coefficients is as good as that compared to the channel estimation using time-domain deconvolution.

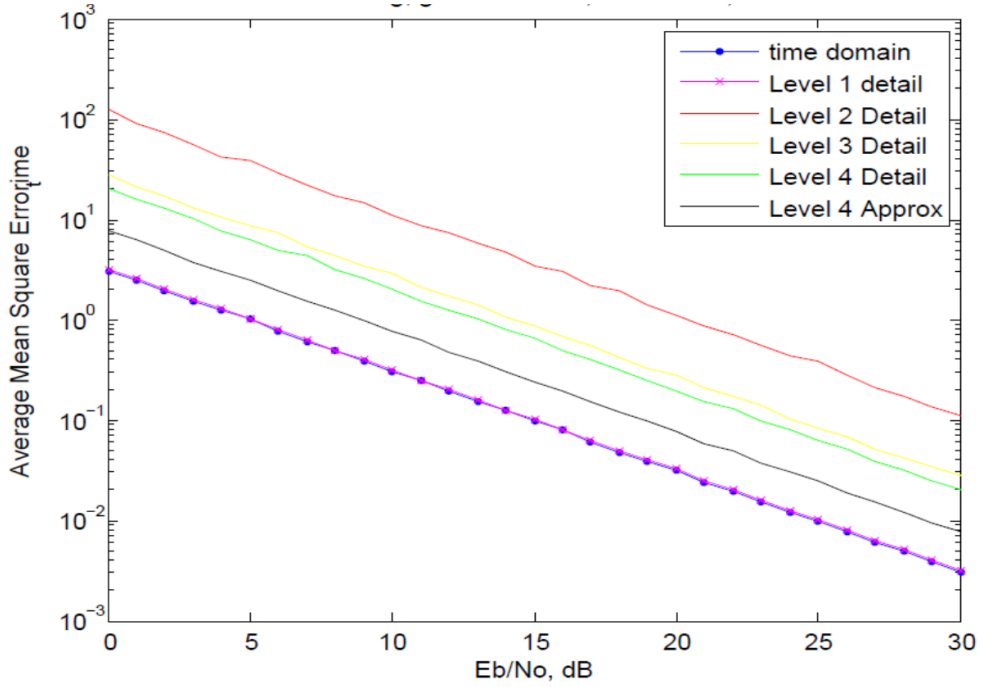

Figure 5.5 Channel impulse response estimation errors for the fast fading Gaussian power delay profile case; Haar wavelet.

Channel estimation MSE plots for the other wavelets are plotted below as follows. The other wavelets used in the simulation experiments are Daubechies2, Daubechies3, Daubechies4.

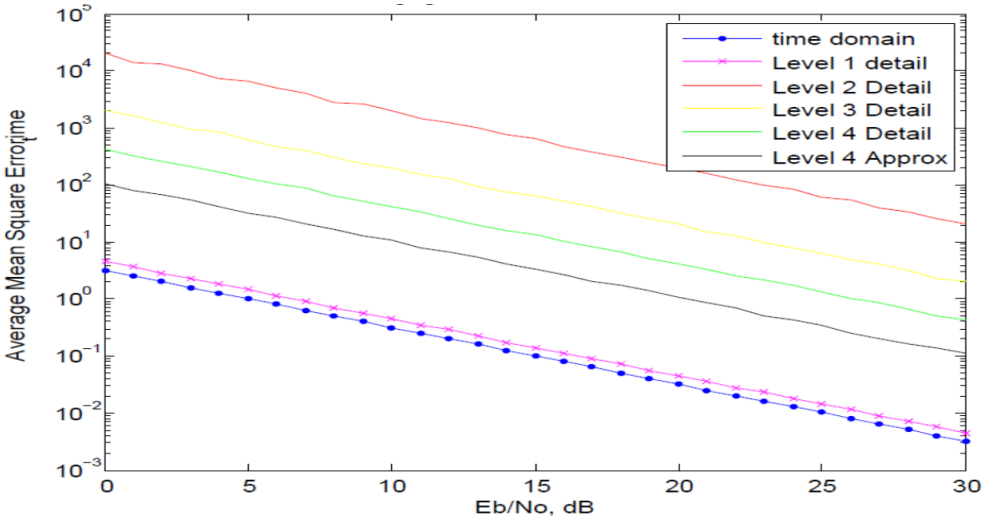

Figure 5.6 Channel impulse response estimation errors for the fast fading Gaussian power delay profile case; Db2 wavelet.

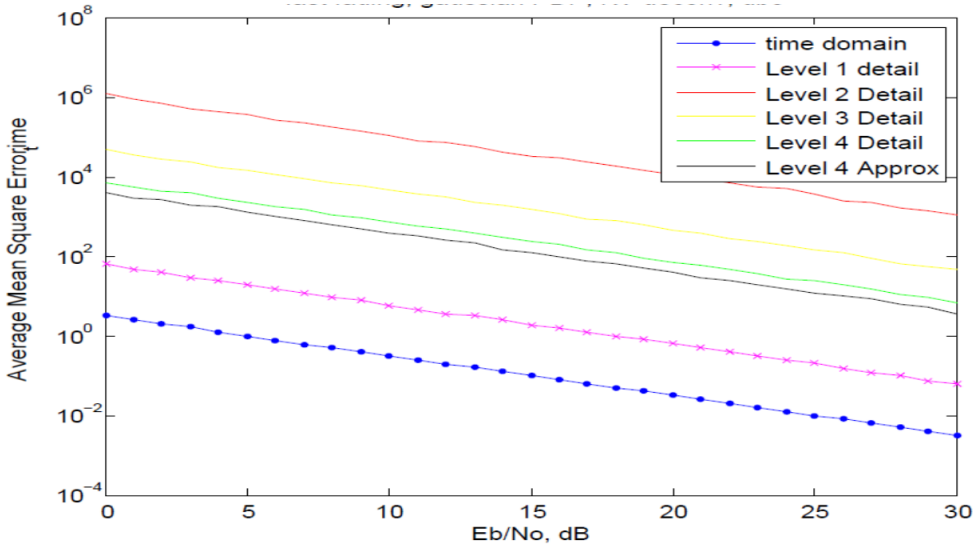

Figure 5.7 Channel impulse response estimation errors for the fast fading Gaussian power delay profile case; Db3 wavelet.

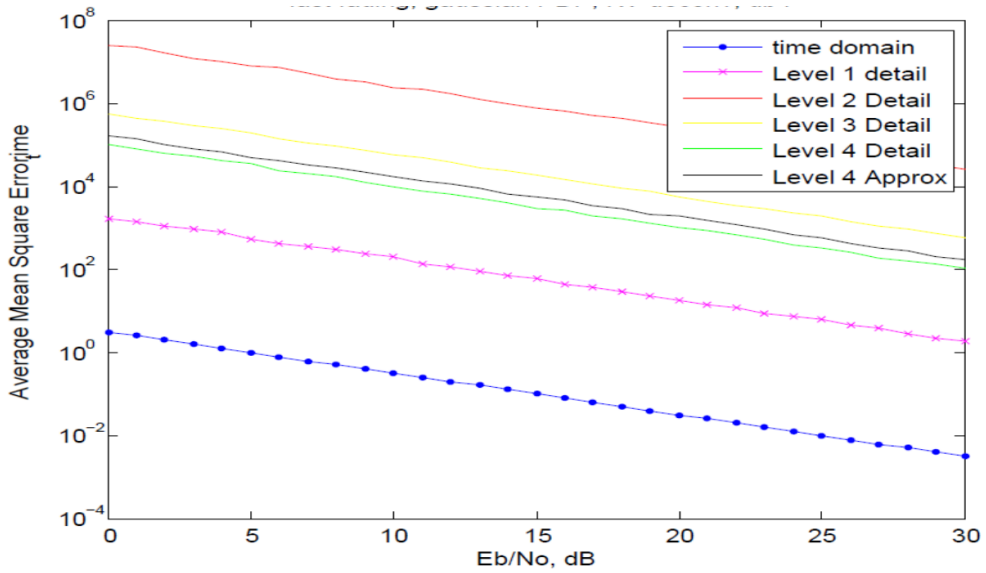

Figure 5.8 Channel impulse response estimation errors for the fast fading Gaussian power delay profile case; Db4 wavelet.

5.3.2 Channel 2: Exponential power delay profile

The second channel PDP considered in this study has the functional form of an exponential decay. The PDP is defined as follows

$$\phi_c(t) = \begin{cases} \frac{1}{\tau} e^{-(t/\tau)} & t \geq 0 \\ 0 & otherwise \end{cases} \tag{5.28}$$

For this channel the same two cases of fading are considered i.e., one with fast fading where the value of d is 0.2 and the other is slow fading where the value of d is set to 2.5. The duration of the channel impulse response was fixed at 5 sec. The values of the impulse response were generated at a rate of 10 samples/s, which resulted in the length of the discretized impulse response being 50 samples.

The plot of the channel PDP's are shown in the following figures.

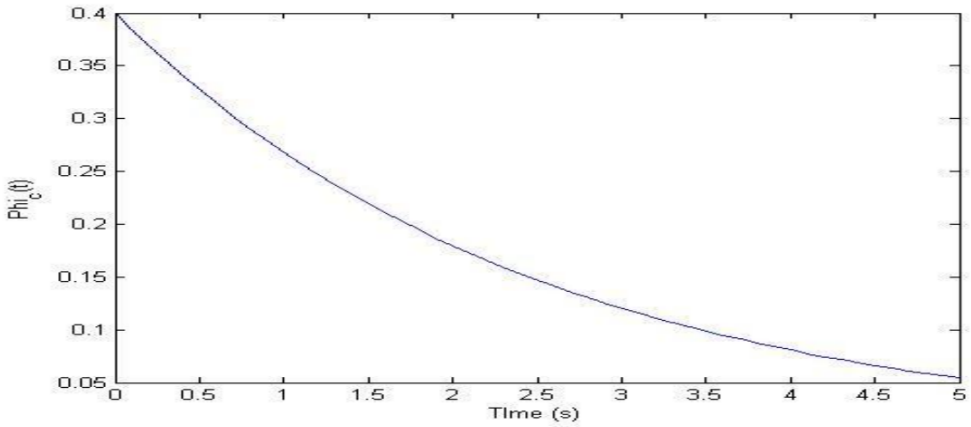

Figure 5.9 Exponential channel PDP for slow fading.

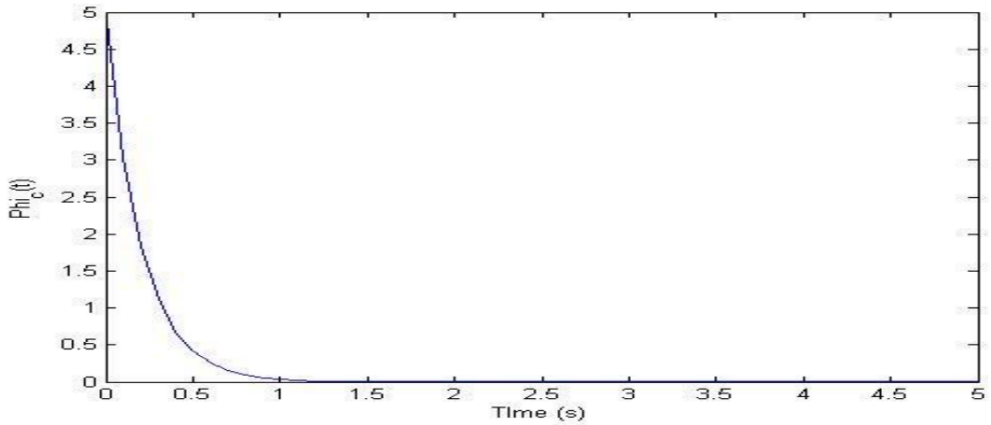

Figure 5.10 Exponential channel PDP for fast fading.

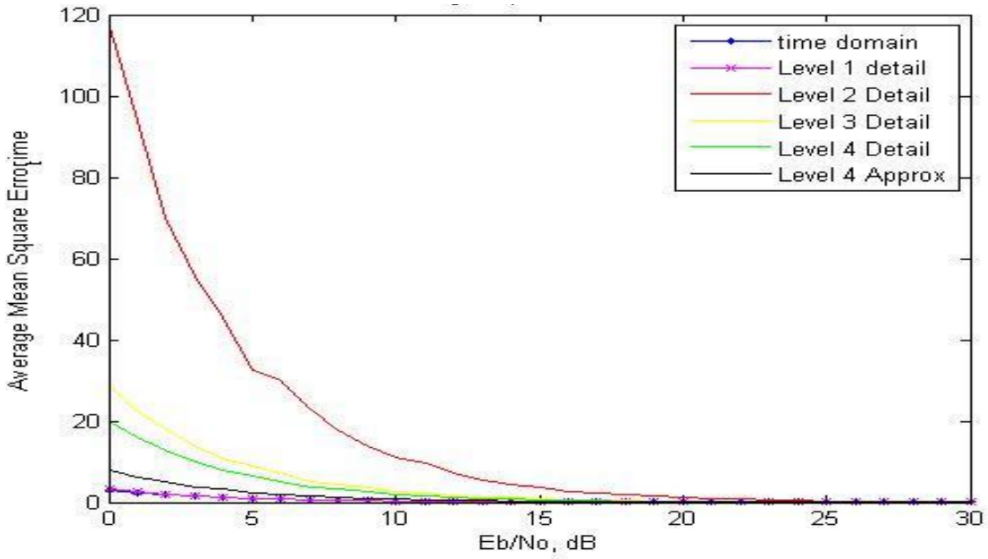

Figure 5.11 Channel impulse response estimation errors for the fast fading Exponential power delay profile case; Haar wavelet.

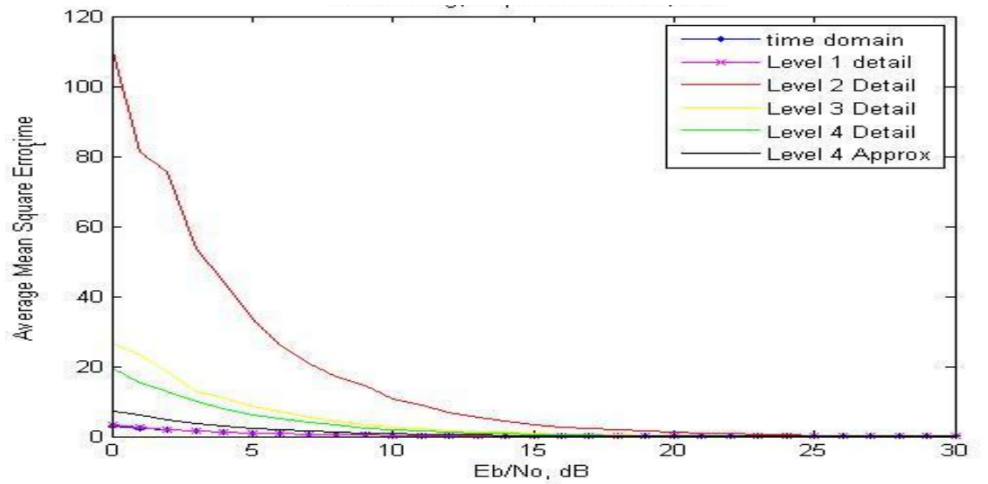

Figure 5.12 Channel impulse response estimation errors for the slow fading Exponential power delay profile case; Haar wavelet.

In the experiment for this type of channel, the channel estimates were calculated using the Haar wavelet for both the fast and slow fading cases. The estimates were calculated at four levels of resolution. Hence, there are totally five estimates which includes four of them from the DWT Detail coefficients at each of the four levels of resolution and one from the DWT Approximation coefficients at the last level of resolution.

Chapter 6

Discrete wavelet transform-based adaptive equalization

6.1 Equalization using DWT

Least mean squares is a well defined equalization procedure which equalizes the channel output depending on the channel changes by adaptively modifying the equalizer weights. The idea here is to perform the adaptive equalization in the wavelet domain. The main approach is to develop a DWT-based Adaptive Equalizer and compare its performance with that of a well known adaptive equalizer (LMS Equalizer) in terms of error probability.

6.2 Strategy for DWT-based adaptive equalization

The block diagram for DWT-LMS algorithm is given in Figure 6.1. In the figure, the following parameters are shown:

1. $p(n)$ is the transmitted pilot signal.
2. $q(n)$ is the ISI introduced AWGN distorted received pilot signal.
3. $B(z)$ is the equalizer filter block.
4. $\hat{q}(n)$ is the pilot equalized output signal at any iteration.
5. DWT is a block which performs discrete wavelet transform of the incoming signal.
6. $p_d(n)$ is the DWT Detail coefficients of p(n) at one level of resolution.
7. $e(n)$ is the error signal between $p_d(n)$ and y(n).
8. y(n) is the unknown ISI introduced AWGN distorted signal to be equalized.
9. $\hat{x}(n)$ is the equalized output signal of y(n).

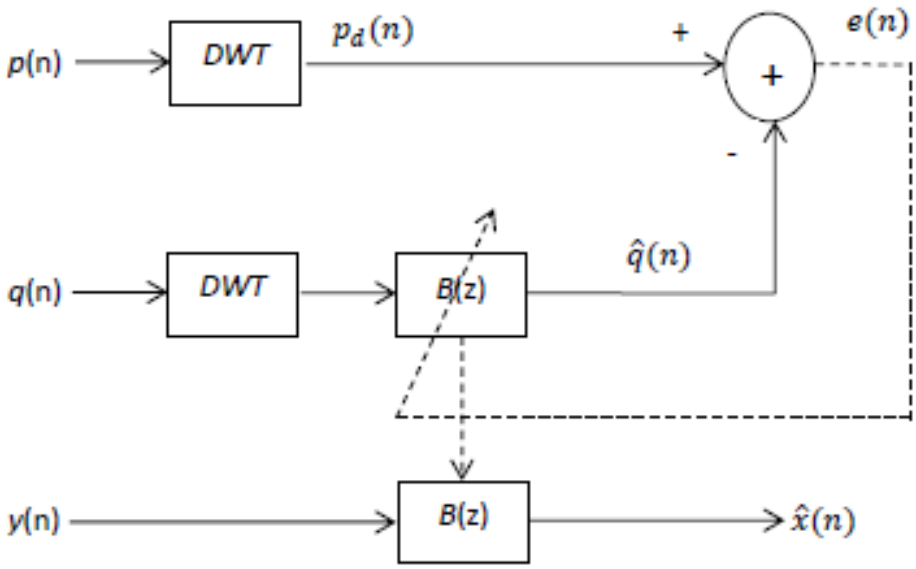

Figure 6.1 Strategy for DWT-based adaptive equalization.

In the training phase, the transmitted pilot signal, i.e., $p(n)$ and the ISI introduced, AWGN distorted copy of the pilot signal, i.e., $q(n)$ are DWT analyzed to one level of resolution. The Detail coefficients of both the signals are obtained at the first level of resolution. These Detail coefficients are used as inputs to the adaptive filter. In this strategy the weights of the adaptive filter are updated by the LMS algorithm as explained in Section 2.3. Once the training phase is completed and the weights of the equalizer filter $B(z)$ is obtained, the signal to be equalized is passed through the equalizer filter, $B(z)$ to obtain an estimate of original transmitted signal $x(n)$, i.e., $\hat{x}(n)$.

6.3 Computer simulation experiments

Simulation experiments are performed for the following scenarios:

1. Two Channel PDP models.
2. Addition of white Gaussian noise to every signal and introduction of ISI.
3. Use of the the Haar, db2, db3, and db4 wavelets for channel estimation.

In each experiment, the test signal is convolved with the channel impulse response, intersymbol-interference is introduced in the convolved signal and a additive white Gaussian noise with a double-sided Power Spectral Density (PSD) of $\frac{N_0}{2}$ is added to the received signal. BPSK is the modulation used in the experiments.

The parameter $\frac{E_b}{N_0}$ is used throughout this work to provide a relative measure of the energy contained in every bit that is transmitted. In each experiment the error probability employing both LMS and DWT-based LMS adaptive equalizers is computed. A total of 1000 data bits and 250 training bits are transmitted for each value of $\frac{E_b}{N_0}$. The experiment is simulated for 25 Monte Carlo simulations. An average of the resulting ensemble of the probability of error's for each value of $\frac{E_b}{N_0}$ is then computed and graphed. The simulations are performed for each of the Haar, db2, db3 and db4 wavelets.

6.4 Results

The results are provided for the following two PDP channel:

1. Slow fading Gaussian PDP channel.
2. Slow fading Exponential PDP channel.

6.4.1 Channel 1: Slow fading Gaussian power delay profile

The Gaussian PDP is defined as

$$\phi_c(t) = \frac{1}{\sqrt{2\pi\tau}} exp(\frac{-(t/\tau)^2}{2}) \tag{6.1}$$

In (6.1), τ is known as "the root mean square delay spread" and is defined as,

$$\tau = dT_{sym} \tag{6.2}$$

Here, d is the normalized delay time and T_{sym} is the baseband symbol period and is set to 1 second. The PDP of the Gaussian channel $\tau = 3$ Sec is shown below in Figure 6.2.

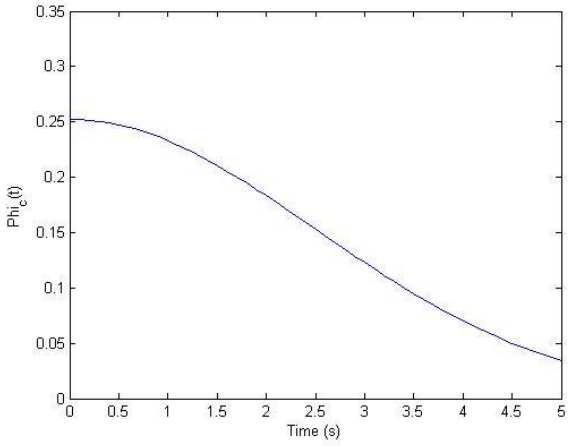

Figure 6.2 Gaussian power delay profile for delay spread of 3 seconds.

Figures 6.3 to Figure 6.6 plot the probability of error versus $\frac{E_b}{N_0}$ for LMS Adaptive Equalizer and DWT-based LMS Adaptive Equalizer in a Gaussian channel PDP model.

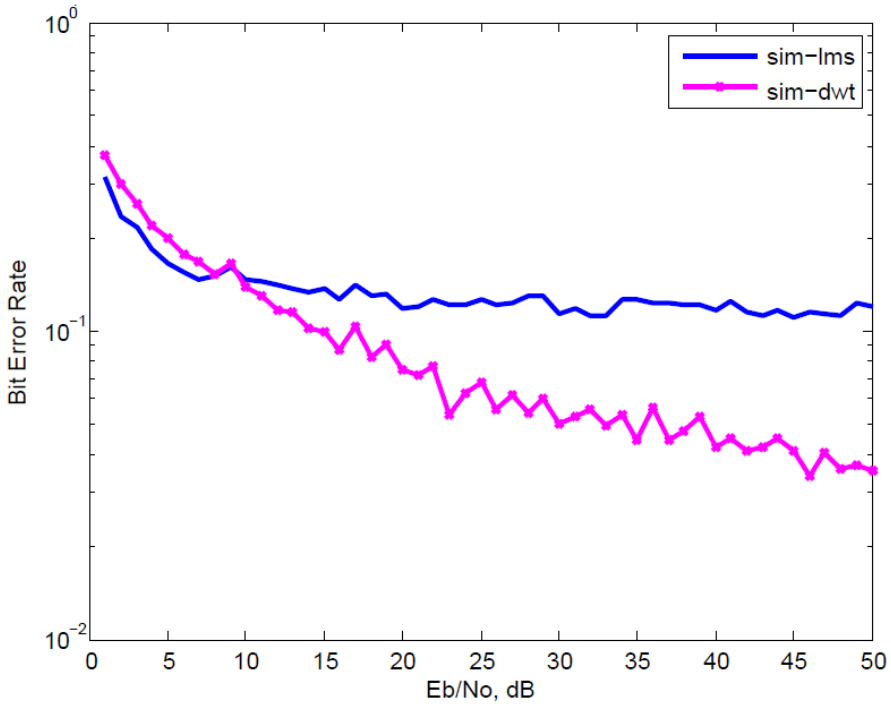

Figure 6.3 Error probability vs SNR for LMS and DWT-LMS equalizers using the Haar wavelet in Gaussian PDP channel.

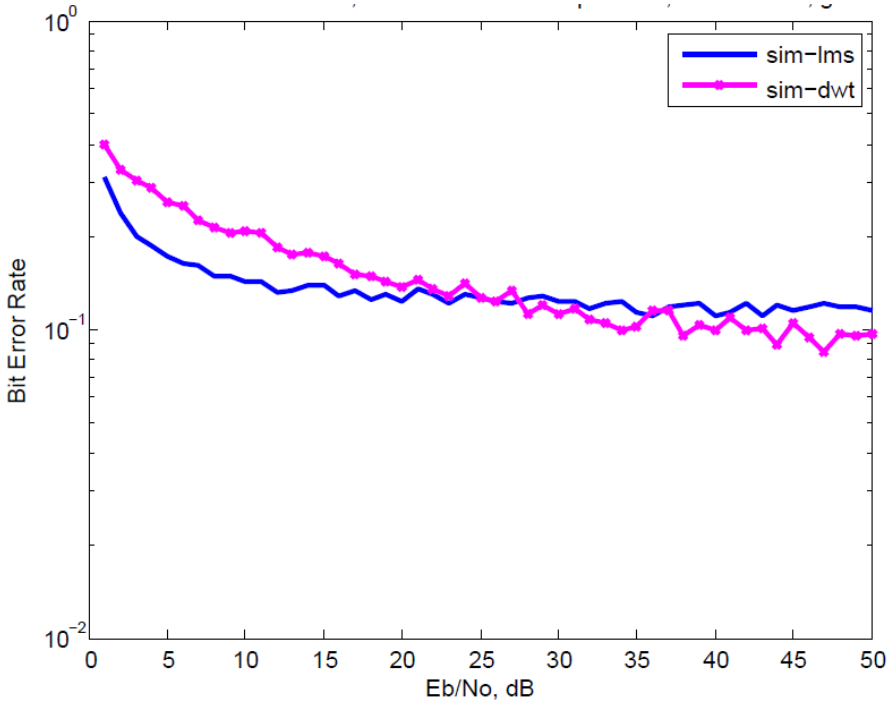

Figure 6.4 Error probability vs SNR for LMS and DWT-LMS equalizers using db2 wavelet in Gaussian PDP channel.

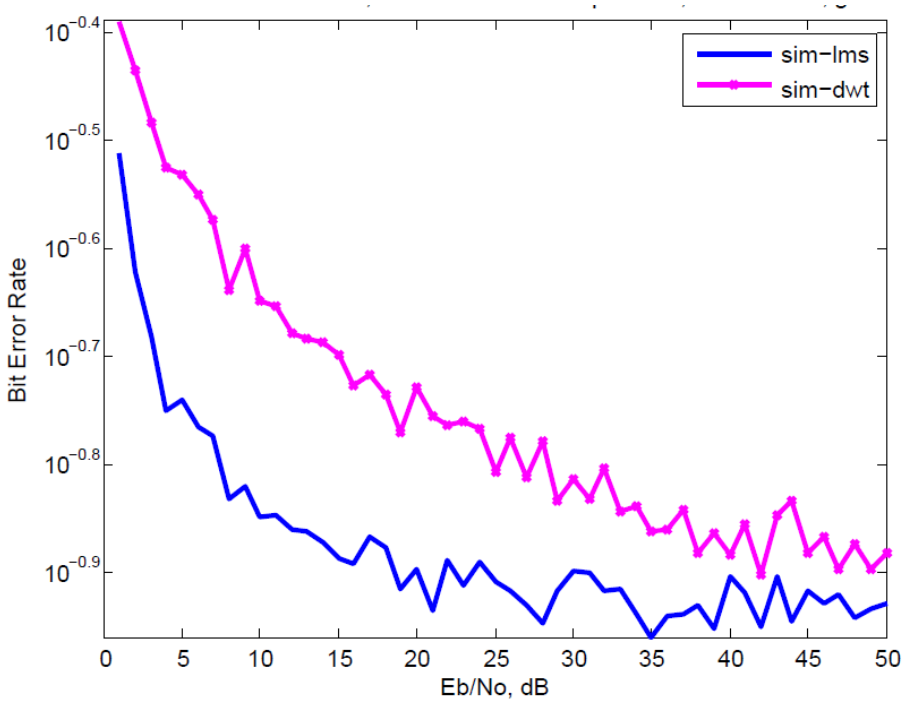

Figure 6.5 Error probability vs SNR for LMS and DWT-LMS equalizers using db3 wavelet in Gaussian PDP channel.

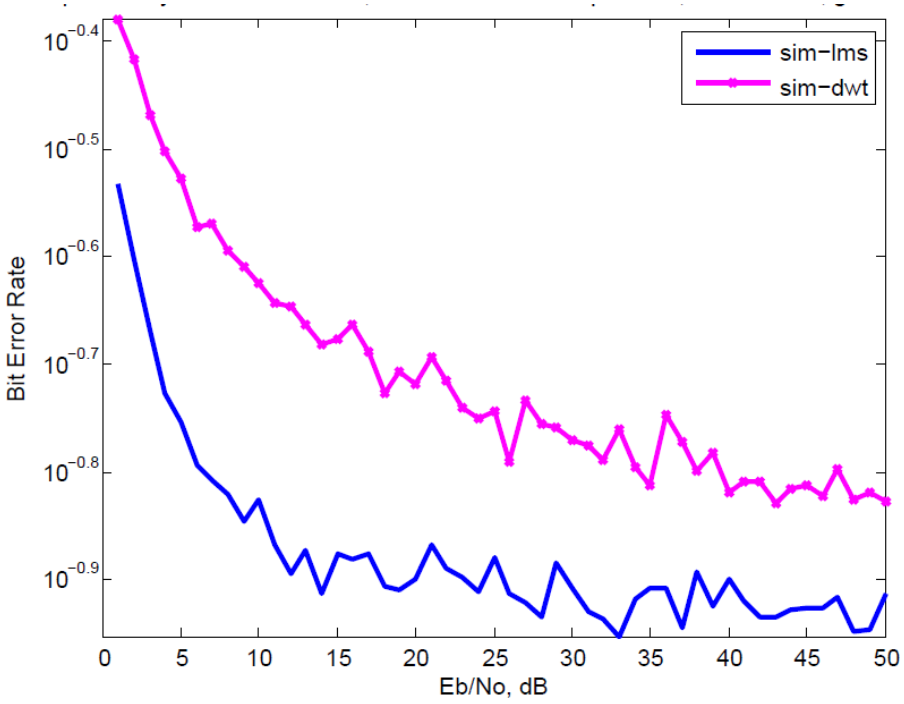

Figure 6.6 Error probability vs SNR for LMS and DWT-LMS equalizers using db4 wavelet in Gaussian PDP channel.

6.4.2 Channel 2: Slow fading Exponential power delay profile

The second channel considered here has the functional form of Exponential decay. The PDP is defined as follows

$$\phi_c(t) = \frac{1}{\tau} e^{\frac{-t}{\tau}} \quad \forall\, t \geq 0 \tag{6.3}$$

where τ is RMS delay spread. The Exponential PDP channel having a delay spread of 3 seconds is in Figure 6.7. Figure 6.8 to Figure 6.11 plot the probability of error versus $\frac{E_b}{N_0}$ for the LMS adaptive equalizer and the DWT-based LMS adaptive equalizer in a Exponential PDP channel model. Here, the Haar, db2, db3 and db4 wavelets are employed.

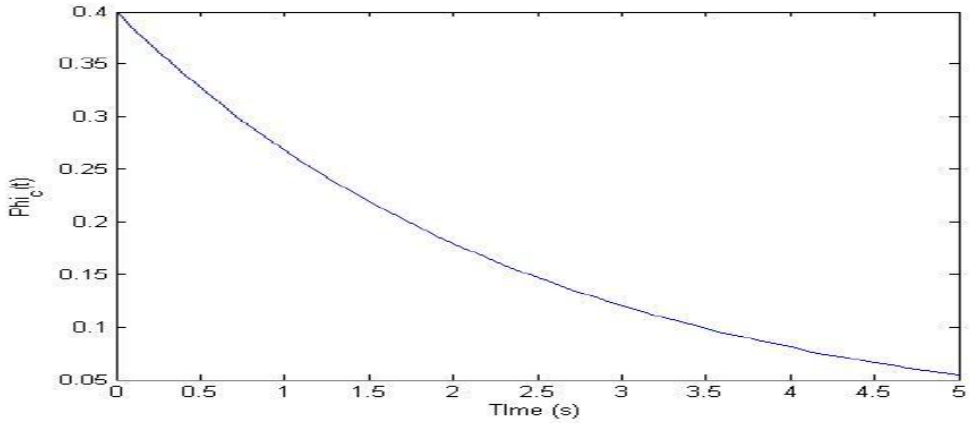

Figure 6.7 Exponential PDP for RMS delay spread of 3 seconds.

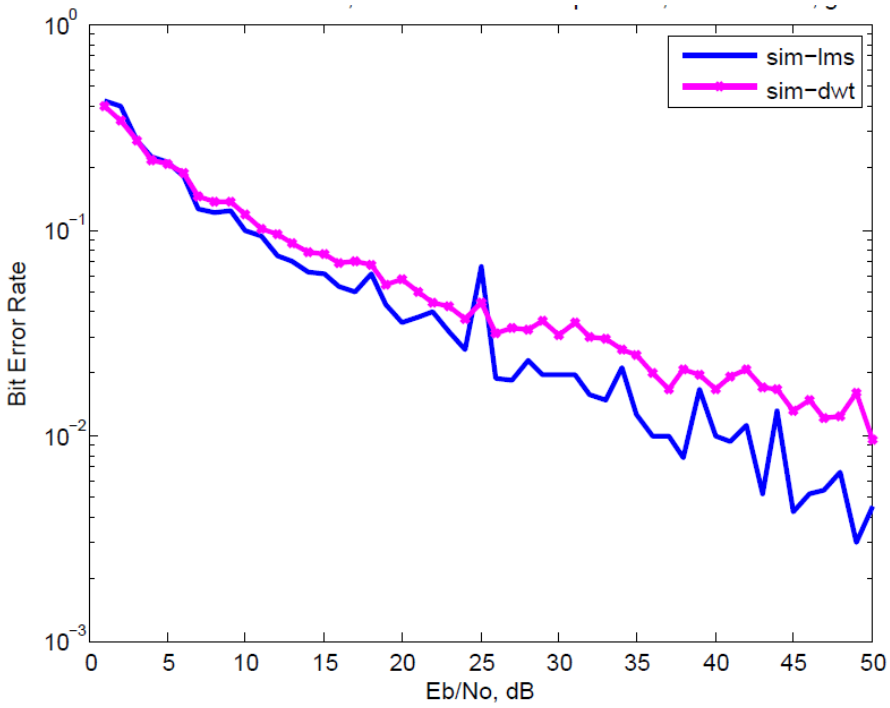

Figure 6.8 Error probability vs SNR for the LMS and DWT-LMS equalizers using the Haar wavelet in Exponential PDP channel.

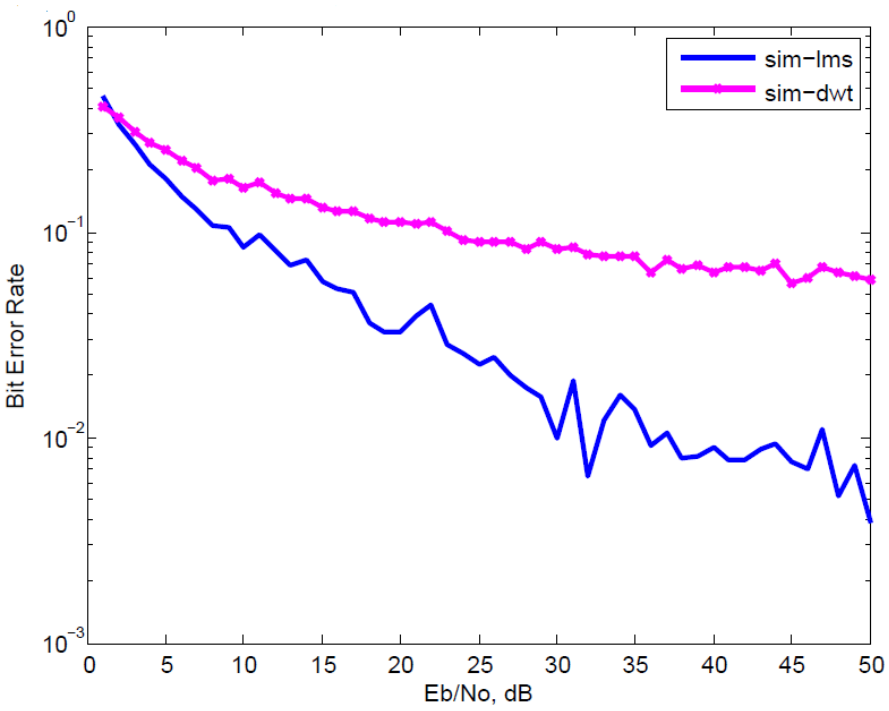

Figure 6.9 Error probability vs SNR for the LMS and DWT-LMS equalizers using db2 wavelet in Exponential PDP channel.

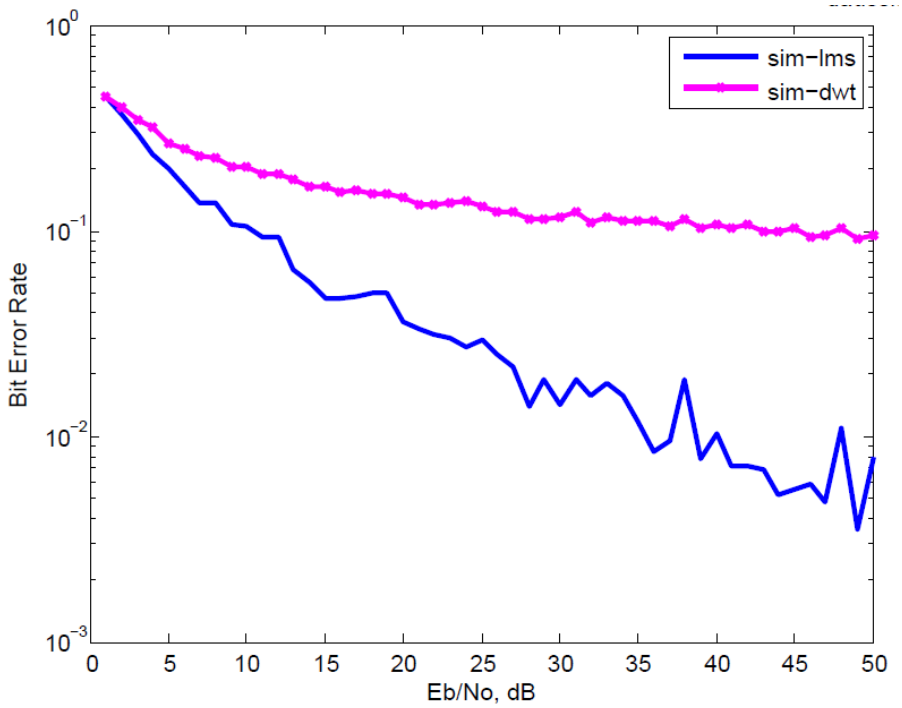

Figure 6.10 Error probability vs SNR for the LMS and DWT-LMS equalizers using db3 wavelet in Exponential PDP channel.

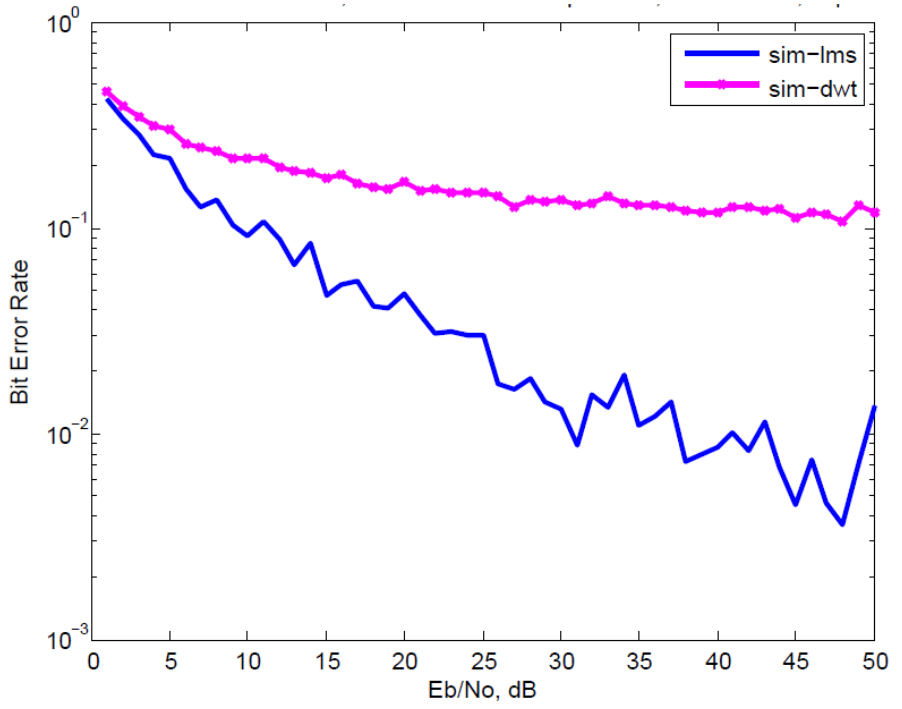

Figure 6.11 Error probability vs SNR for the LMS and DWT-LMS equalizers using db4 wavelet in Exponential PDP channel.

6.5 Observations

From the results, it can be seen that the bit error probability curve performs better when the Haar wavelet is used when compared to the other wavelets in Daubechies family i.e., db2, db3 and db4. Specifically in the case of Gaussian channel, the bit error performance of the DWT-LMS Adaptive Equalizer is better when compared to LMS Adaptive equalizer when the Haar wavelet is used. In the Exponential channel, the bit error rates were considerable lower for both the LMS and DWT-LMS equalizers when compared to the other channel, i.e., Gauusian PDP channel. Even in the case of the Gaussian channel with the Haar wavelet, the bit error rates of both the equalizers are comparatively similar.

Chapter 7

Conclusions

This chapter concludes the thesis and provides a detailed summary and possible extension of this thesis in the future.

In the first section, a summary of the salient features for each of the research topics in this thesis is highlighted. The second section, Future work tells about the limitations in the present thesis and provides an insight for the ideas that can be extended beyond this thesis.

7.1 Summary

In the response of the objectives mentioned in Section 1.2, the following observations are in order:

1. It is possible to determine the time domain impulse response of the channel using the wavelet transform.

2. An algorithm has been implemented for Wavelet-based channel estimation.

3. It is been proved that the fading effects of the channel can be equalized using DWT-based channel equalization.

4. An algorithm has been developed for the Adaptive Equalization of channel fading effects using the Discrete wavelet transform.

Forward merge approach and forward merge approach to convolution with polyphase filtering have been discussed in Chapter 4. Using these approaches convolution in the discrete wavelet domain is made possible. These methods have been described

using theoretic concepts and has also been represented in the form of filter bank block diagrams.

The deconvolution procedure uses partial DWT analysis. In this, the undecimated wavelet coefficients are used for the purpose of deconvolution which gives the channel impulse response. These coefficients can be obtained at various levels of resolution. The resulting methodologies have been applied to different types of channels and each channel is defined to reflect the fast fading and slow fading scenarios. Additive white Gaussian noise is also added to these corrupted signals. All the simulation experiments have been carried out using different wavelet families. It has been found that the channel impulse response can be obtained by applying the deconvolution procedure to the wavelet coefficients at any one level of resolution and the accuracy of the estimate varies randomly from on level to other. The observations show that the estimation errors decreases as the signal power is increasing compared to the noise power. The best channel estimates are obtained from the detail coefficients at the first level of resolution in both the channels.

The well-know adaptive equalization algorithm LMS has been implemented using the DWT. In this strategy both the transmitted and received copies of the pilot signal are DWT analyzed to one level of resolution. The detail and the approximation coefficients are obtained by passing the DWT analyzed signal into high pass and low pass filters, respectively. The algorithm uses only the Detail coefficients to be passed into the adaptive filter. The filter weights are derived such that the error between the DWT analyzed signals of both the original pilot and the channel corrupted pilot minimizes. The experiments performed based on this algorithm involves two different channel models, each representing both slow and fast fading. From the results, it has been seen that error probability curves for the Haar wavelet outperforms the other wavelets in the Daubechies family. The performance of DWT LMS algorithm is better than the original LMS algorithm performance in the case of a Gaussian channel when the Haar wavelet is used. In the case of the Exponential channel model, the bit error probability curves for DWT-LMS are not as good compared to the performance obtained using the

traditional LMS adaptive equalization method.

7.2 Future work

All the experiments performed in this research study involves the use of only Daubechies wavelets. A research topic in the future can be to investigate the experiments with other sets of wavelets.

As noted from the literature survey, there is an existing automatic modulation recognition algorithm. Hence, a possible research topic would be to develop a de-noising algorithm, so an entire wavelet platform can be created which will comprise of channel estimation, adaptive channel equalization, Automatic modulation recognition and a de-noising algorithm, hence making a complete wavelet platform for an agile transceiver. It is shown that the DWT-LMS method with the Haar wavelet has lower bit error rates than the traditional LMS method, however, the convergence property is not addressed in this research work. Thus, another topic for future work may be a further investigation on the convergence properties of the newly developed DWT-LMS adaptive equalization algorithm. The DWT-LMS algorithm considered in this study, makes use of only the Detail coefficients at one level of resolution. The natural progression of this research work would be to extend this algorithm to make use of both Detail and Approximation coefficients at more levels of resolution.

Bibliography

[1] Canute Vaz. *Estimation and equalization of communications channels using wavelet transforms.* PhD thesis, Rutgers University, Graduate School-New Brunswick, 2010.

[2] Canute Vaz, K. Ho, D. Daut, and Y. Ge. Estimation of communications channels using discrete wavelet transform-based deconvolution. Gaithersburg, MD, USA, 2013.

[3] John G. Proakis. *Digital Communications.* McGraw-Hill, New York, 5 edition, 2008.

[4] Athanasios Papoulis and S. Unnikrishna Pillai. *Probability, random variables, and stochastic processes.* Tata McGraw-Hill Education, 2002.

[5] Robi Polikar. The wavelet tutorial. Rowan University, Glassboro, NJ, 1996.

[6] Brani Vidakovic and Peter Mueller. Wavelets for kids. *Instituto de Estadística, Universidad de Duke*, 1994.

[7] Fuqin Xiong. Digital modulation techniques. 2000.

[8] Equalization. `http://www.winlab.rutgers.edu/~crose/421_html/equalization.pdf`.

[9] Adaptive Equalizer. `http://www.srmuniv.ac.in/sites/default/files/files/adaptive_equalizer.pdf`.

[10] Tao Li, Qi Li, Shenghuo Zhu, and Mitsunori Ogihara. A survey on wavelet applications in data mining. *ACM SIGKDD Explorations Newsletter*, 4(2):49–68, 2002.

[11] Raghuveer M. Rao and Ajit S. Bopardikar. *Wavelet transforms-introduction to theory and applications.* Addison-Wesley-Longman, MA, 1997.

[12] G. Beylkin. Wavelets, multiresolution analysis and fast numerical algorithms. *Wavelets: theory and applications, ICASE/LaRC Series in Computational Science and Engineering*, pages 182–262, 1991.

[13] Michail K. Tsatsanis and Georgios B. Giannakis. Time-varying system identification and model validation using wavelets. *Signal Processing, IEEE Transactions on*, 41(12):3512–3523, 1993.

[14] Eric Moulines, Pierre Duhamel, J.F. Cardoso, and Sylvie Mayrargue. Subspace methods for the blind identification of multichannel FIR filters. *Signal Processing, IEEE Transactions on*, 43(2):516–525, 1995.

[15] Massimiliano Martone. Wavelet-based separating kernels for sequence estimation with unknown rapidly time-varying channels. In *Signal Processing Advances in Wireless Communications, 1999. SPAWC'99. 1999 2nd IEEE Workshop on*, pages 255–258, Gaithersburg, MD, 1999.

[16] Massimiliano Martone. Wavelet-based separating kernels for array processing of cellular ds/cdma signals in fast fading. *Communications, IEEE Transactions on*, 48(6):979–995, 2000.

[17] G. Tong Zhou, Yongsub Kim, and G.B. Giannakis. Estimation and equalization of time-selective fading channels. In *Signals, Systems, and Computers, 1999. Conference Record of the Thirty-Third Asilomar Conference on*, volume 1, pages 248–252, Atlanta, GA, 1999.

[18] Seyed Mohammad Sajad Sadough, Mahieddine M. Ichir, Pierre Duhamel, and Emmanuel Jaffrot. Wavelet-based semiblind channel estimation for ultrawideband OFDM systems. *Vehicular Technology, IEEE Transactions on*, 58(3):1302–1314, 2009.

[19] Hiroki Harada, Marco Hernandez, and Ryuji Kohno. Channel estimation for

wavelet packet based UWB transmissions. In *Spread Spectrum Techniques and Applications, 2006 IEEE Ninth International Symposium on*, pages 178–182, Yokohama Nat. Univ., 2006.

[20] Hui Luo and Yanda Li. The application of blind channel identification techniques to prestack seismic deconvolution. *Proceedings of the IEEE*, 86(10):2082–2089, 1998.

[21] Feng Liu, Jun Cheng, Jinbiao Xu, and Xinmei Wang. Wavelet based adaptive equalization algorithm. In *Global Telecommunications Conference, 1997. GLOBECOM'97., IEEE*, volume 3, pages 1230–1234, Xidian Univ., Xi"an, China, 1997.

[22] X. Niu. Research of discrete wavelet transform domain adaptive equalization algorithm. In *Signal Processing, 2006 8th International Conference on*, volume 1, PLA University of Science and Technology, 2006.

[23] Nuria González Prelcic, Fernando Pérez González, and M. Jiménez. Wavelet packet-based subband adaptive equalization. *Signal Processing*, 81(8):1641–1662, 2001.

[24] Feng Liu, Jun Cheng, and Xinmei Wang. A new kind of equalizer based on orthonormal wavelets. *Journal of Electronics (China)*, 16(1):38–43, 1999.

[25] A. Minayi Jalil, Hamidreza Amindavar, and Farshad Almasganj. Subband blind equalization using wavelet filter banks. In *Circuits and Systems, 2005. ISCAS 2005. IEEE International Symposium on*, pages 5730–5733, Tehran, Iran, 2005.

[26] Dimitri Cariolaro and Lorenzo Favalli. Recovery of ISI channels using multiresolution wavelet equalization. In *Communications, 2002. ICC 2002. IEEE International Conference on*, volume 1, pages 74–78, Pavia Univ., Italy, 2002.

[27] Stephane G. Mallat. Multiresolution approximations and wavelet orthonormal bases of $L^2(R)$. *Transactions of the American Mathematical Society*, 315(1):69–87, 1989.

[28] Stephane G. Mallat. *A wavelet tour of signal processing.* Academic Press, 1999.

[29] Gregory Beylkin, R. Coifman, and V. Rokhlin. Wavelets in numerical analysis. *Wavelets and their applications*, 181, 1992.